Submitted to Physical Review C

RECEIVED
LAWRENCE
RADIATION LABORATORY

LBL-1606
Preprint c.1

LIBRARY AND
DOCUMENTS SECTION

# NUCLEAR SPECTROSCOPY STUDIES ON THE ALPHA DECAY OF $^{235}$Np AND BETA DECAY OF $^{231}$Th

E. Browne and F. Asaro

January 1973

Prepared for the U. S. Atomic Energy Commission
under Contract W-7405-ENG-48

For Reference

Not to be taken from this room

LBL-1606
c.1

## DISCLAIMER

This document was prepared as an account of work sponsored by the United States Government. While this document is believed to contain correct information, neither the United States Government nor any agency thereof, nor the Regents of the University of California, nor any of their employees, makes any warranty, express or implied, or assumes any legal responsibility for the accuracy, completeness, or usefulness of any information, apparatus, product, or process disclosed, or represents that its use would not infringe privately owned rights. Reference herein to any specific commercial product, process, or service by its trade name, trademark, manufacturer, or otherwise, does not necessarily constitute or imply its endorsement, recommendation, or favoring by the United States Government or any agency thereof, or the Regents of the University of California. The views and opinions of authors expressed herein do not necessarily state or reflect those of the United States Government or any agency thereof or the Regents of the University of California.

# NUCLEAR SPECTROSCOPY STUDIES ON THE ALPHA DECAY OF $^{235}$Np AND BETA DECAY OF $^{231}$Th

E. Browne and F. Asaro

Lawrence Berkeley Laboratory
University of California
Berkeley, California 94720

January 1973

## ABSTRACT

The alpha decay of $^{235}$Np has been studied by quantitative α singles and α-γ coincidence techniques, and the beta decay of $^{231}$Th by quantitative γ ray singles and γ-γ two parameter coincidence measurements with semiconductor detectors. Rotational bandheads in $^{231}$Pa at 102.30, 174.10 and 183.47 keV are given the Nilsson assignments ($\Omega\ \pi(N\ n_z\ \Lambda)$) 3/2 + (651), 5/2 - (523), and 5/2 + (642). Decay schemes for $^{235}$Np and $^{231}$Th are presented as well as a transition intensity balance for $^{231}$Th which includes beta branchings. Energy level spacings and α, β, and γ transition probabilities are interpreted in terms of a strong Coriolis interaction among the even parity rotational bands and admixtures in the wave functions are given for the observed levels.

# I. INTRODUCTION

The low-lying energy levels of $^{231}$Pa and $^{233}$Pa are of particular interest because of the strong Coriolis forces between a number of states, and the opportunity to see the effect of these forces not only on the energy level spacings but also on the α, β, and γ transition probabilities.

This study on $^{231}$Pa energy levels was prompted by an earlier investigation of $^{237}$Np α decay[1] which demonstrated distortions in the energy level spacings and in the α and γ transition probabilities. Concurrent with the present study Hoekstra and Wapstra[2] in their paper on the energy levels of $^{233}$Pa also suggested $^{231}$Pa might be similar. The study of $^{235}$Np alpha decay is complicated by the minute alpha branching of this predominately electron capture activity.

In the present work, which has been reported in preliminary fashion earlier,[3,4,5] quantitative α-γ coincidence measurements were made on $^{235}$Np and quantitative γ ray singles and γ-γ coincidence measurements on $^{231}$Th. Four new energy levels are observed and two more are assigned different energies. Reassignment of Nilsson quantum numbers are made for the states at 84.17 and 183.47 keV and a new assignment is made for the rotational bandhead at 174.10 keV. An intensity balance is performed for both β and γ transitions in $^{231}$Th decay.

The even parity energy levels in $^{231}$Pa are interpreted with a complete Coriolis calculation and admixtures in the wave functions are obtained for each observed state. Although the experimental ratios of the α, β, and γ transition probabilities to the even parity states are rather unusual, they agree reasonably well with calculated results if Coriolis-mixed wave functions are used.

## II. SOURCE PREPARATIONS

$^{235}Np$ was produced by bombarding 1 gm of highly enriched (94.4%) $^{235}U$ with 18 MeV deuterons for 978 μ amp hours in the 88 inch cyclotron at the Lawrence Berkeley Laboratory. The uranium target was dissolved in 10 M HCl and adsorbed onto a Dowex AG1-X8 anion exchange column. Washes with more 10 M HCl removed the fission products, and elution of the column with 2.7 M HCl removed the Np and Pu and left U on the column. The Np-Pu fraction was loaded onto another Dowex AG1-X8 anion column in 10 M HCl - 0.1 M HI solution, washed with the same solution to remove Pu, and the Np eluted off the column with 2.7 M HCl. The Np fraction was loaded onto a Dowex AG50-X12 cation exchange column in 0.1 M HCl, and then the Np was stripped off in 10 M HCl. Any Pa remained on the column. The purified Np fraction contained 22 h $^{236}Np$ which grew $^{236}Pu$, and made it necessary to repeat the purification from Pu two weeks later.

The sample was purified from extraneous mass by absorption onto a Dowex AG50-X12 cation exchange column in 0.1 M HCl followed by elution with 2 M and 10 M HCl. At the end of the chemical purifications, a very thin source of 180 α dis/min was prepared by electroplating the purified neptunium onto a 0.001" Pt foil. Another source of 500 α dis/min was electroplated onto a 0.0001" Ni foil. Both sources contained $^{237}Np$ as an impurity.

$^{231}Th$ was prepared by bombarding 500 μgms of $^{230}Th$ with neutrons in the University of California Triga research reactor. The Th target was dissolved in 8 M $HNO_3$ with a drop of HF and the solution was adsorbed onto a Dowex AG1-X8 anion exchange column. The column was washed with 8 M $HNO_3$ which removed the rare earths, and then the Th was stripped from the column with 0.1 M $HNO_3$. $^{143}Ce$ and $^{140}La$, however, were not completely separated from the thorium by this chemistry.

There was no attempt to separate the rare earths in the sources used for the $\gamma$-$\gamma$ coincidence measurements. $^{233}$Pa, which resulted from small amounts of $^{232}$Th in the target, was adsorbed onto a Dowex AG1-X8 anion exchange column in 10 M HCl as the Th washed through. After the chemical purification the Th solutions were evaporated to dryness on 0.001" Ni foils.

## III. EQUIPMENT AND CALIBRATIONS

### A. $^{235}$Np Alpha Singles Measurements

The alpha spectrum of $^{235}$Np was measured with a 6 mm diameter Au-Si surface barrier detector with a full-width-at-half-maximum (FWHM) of 14.5 keV. Because of spurious α-particle groups due to coincidences between the main α-particle groups and conversion electrons from the intense 84.2 keV transition, there was some difficulty in observing low-intensity α-particle groups of $^{235}$Np between 5.022 and 5.105 MeV.

A magnetic field of several thousand gauss applied perpendicular to the emitted conversion electrons made the spurious α-particle groups negligible while maintaining the detection geometry of 3.5%. The output of the α-particle detector, which was operated at room temperature, was fed through a charge-sensitive preamplifier and then through various amplifiers to a multi-channel pulse-height analyzer.

Energy calibrations were made with the $^{237}$Np impurity in the source and with an external source of $^{240}$Pu. All the α particle energies are relative to 4.787 MeV for $\alpha_{86}$ in $^{237}$Np[6] and, 5.123 and 5.168 MeV for $^{240}$Pu[7] $\alpha_{45}$ and $\alpha_0$ respectively.

### B. $^{235}$Np α-γ Coincidence Measurements

α particles were detected with a 1 cm diameter Au-Si surface barrier detector cooled to -20°C. The source was 3 mm away from the detector and the FWHM was ≃ 25 keV. The total α-spectrum as well as that part used as the coincidence gate were recorded in a 400 channel pulse height analyzer during each α-γ coincidence experiment in order to test for any change in the electronic gain of the α-particle detector system.

The γ-ray spectra were detected with a 5 cc Ge(Li) detector with a FWHM of 2 keV at 84 keV. The singles γ-ray spectrum was gain-stabilized at the same time as the coincident γ radiations were accumulated in the 400 channel pulse-height analyzer.

The resolving time of the coincidence circuit was 80 nsec. The accidental rate, caused mainly by the U-X rays associated with the electron capture decay of $^{235}$Np, was determined with an additional 10 μsec delay on the γ-ray side and a pulse generator of known frequency on the α-particle side. The shape of the prompt curve of this apparatus and the efficiency as a function of the γ-ray energy were determined from α-γ coincidence measurements with $^{249}$Cf. The absolute photopeak efficiency of the Ge(Li) detector as a function of the γ-ray energy was measured with γ-ray standards of known disintegration rates supplied by the International Atomic Energy Agency in Vienna.

### C. $^{231}$Th Singles Gamma Ray Measurements

The γ-ray spectrum of $^{231}$Th was measured with a high resolution Ge(Li) detector with a FWHM of 670 eV at 90 keV. The output of the detector was fed into a preamplifier[8] with a cooled field-effect transistor for the first stage, a high counting-rate amplifier,[8] a gain stabilizer,[9] and finally a 4,096 channel pulse-height analyzer. The data from the analyzer memory was stored on magnetic tape and later plotted by computer.

### D. $^{231}$Th γ-γ Coincidence Measurements

γ rays were detected with two 5 cc Ge(Li) detectors with a FWHM of 1.3 keV at 122 keV. The source was mounted in an anti-Compton Ag collimator[5]

to absorb γ rays with energies sensibly lower than 150 keV caused by Compton scattering in the detectors.

The electronic equipment used in this work is conventional and has been described elsewhere.[5] The γ rays from the two detectors were fed eventually into a two-parameter coincidence set-up of 1600 × 1600 channels. The coincidence events were stored temporarily in the memory of a 4,096 channel pulse height analyzer and then transferred to a magnetic tape. The γ-ray spectrum from one detector in coincidence with any desired part of the γ-ray spectrum from the other detector could be determined by computer analysis of the magnetic tape.

The resolving time of the coincidence circuit was 0.5 μsec. For most of the measurements the accidental coincidences were about 6% of the true coincidences. The detector relative efficiency as a function of the γ-ray energy was measured with the $^{231}$Th source mounted in the anti-Compton collimator. The γ-ray relative intensities were known from the singles measurements. This was necessary because the size of the source was larger than the central hole in the anti-Compton collimator and γ rays were partially absorbed. The absolute efficiency of the detector was obtained by normalizing one point of the relative efficiency calibration curve to a value, 7.0 ± 0.3%, obtained from the intensity of the 84.2 keV γ ray in the α decay of $^{235}$Np. This normalization was performed using the intensity of the 84.2 keV γ ray in coincidence with $\gamma_{163}$.

## E. Experimental Errors

All the experimental uncertainties are given as two standard deviations unless otherwise indicated in the text.

## IV. $^{235}$Np α-DECAY RESULTS

### A. Singles

The α-particle spectrum of $^{235}$Np is shown in Fig. 1. The best peak shape and tail consistent with the major α-particle component in the sample was developed by trial and error, and then this shape was stripped from each of the observed peaks. This analysis led to 10 α-particle groups assigned to $^{235}$Np.

Four of the ten α groups had been previously observed by Gindler and Engelkemeir[10] and their results along with the present work are presented in Table I. Also included in Table I are our calculated alpha decay hindrance factors using Preston formulas[11] for the theoretical half-lives of the α-particle groups.

The ≈ 10 keV discrepancy in the energies of $\alpha_{186}$ and $\alpha_{250}$ was probably caused by a downward shift of the effective energy of the $^{237}$Np reference peak in the previous work, because the abundant near-lying α-particle groups were not resolved. As the α-particle groups near the main peak in $^{235}$Np are distributed in about the same way as in $^{237}$Np, its energy was relatively unaffected. A discrepancy of a factor of 2 in the intensity of $(\alpha_0 + \alpha_8)$ is probably due to conversion electrons in coincidence with the main α-particle group of $^{235}$Np in the previous work, a possibility indicated by the authors.

### B. α-γ Coincidences

Three coincidence measurements were made between various parts of the $^{235}$Np α-particle spectrum and the γ-ray spectrum. The coincident γ spectra are shown in Fig. 1 and the energies and intensities are given in Table II.

In one experiment the α-particle gate comprised all $^{235}$Np α-particle groups between $\alpha_0$ and $\alpha_{304}$. γ rays of 81.2, 84.2, 102.2, and 110.8 keV are reasonably well defined in this spectrum. Other transitions at 58.5, 125, 165, and 185 keV are less certain. Limits of 0.07% and 0.007% respectively can be placed on the abundance of γ rays at 90 and 174 keV. These limits are of importance in the decay-scheme analysis which will be discussed later. After removing the contribution of accidental coincidences (shown by the dashed lines) from the 90 → 100 keV radiation and smoothing the resulting points, there are peaks at 96 and 92 keV which are presumably the Pa $K_{\alpha_1}$ and $K_{\alpha_2}$ X rays. The intensity of the 110.8 keV transition has had the Pa $K_\beta$ X rays removed as well as accidental coincidences. There is a dubious residue of counts centering at around 92.2 keV which remains after removing all the radiations including Pa-KX rays.

Coincidences between γ rays and α particles in the ranges 4.959 → 5.106 MeV ($\alpha_{113} \rightarrow \alpha_0$) and 4.865 → 4.944 MeV ($\alpha_{186} + \alpha_{171}$) were measured for several weeks. The selected gate regions are indicated in the singles α spectrum shown in Fig. 1. γ rays at 58.5 and 84.2 keV were observed in coincidence with ($\alpha_{113} \rightarrow \alpha_0$). The 84.2 keV γ ray has been previously shown to originate at a 84.2 keV state which receives very high α-particle population.[10] The intensities of these two γ rays have been corrected for the fraction of the decays of the 37 μsec level which did not occur within the resolving time of the circuit. If it is assumed that all the α-particle groups contained in the gate, except ($\alpha_{58} \rightarrow \alpha_0$), populate states which decay through the 84.2 keV level, the intensity of the 84.2 keV γ ray per event populating that level was found to be 6.7 ± 0.5%. The 58.5 keV γ ray presumably originates at the 58 keV state found to be populated

by α particles. This state is populated in high intensity from the 84.2 keV level through a 25.7 keV E1 transition.[12] The intensity of the 58.5 keV γ ray per ($\alpha_{113} \rightarrow \alpha_{84}$) decay is 0.75 ± 0.25%. Therefore, if this state decays only to the ground state, the 58.5 keV transition is almost completely converted, consistent with the E2 assignment from $^{231}$Th decay scheme studies.[13]

The γ-ray spectrum in coincidence with ($\alpha_{186} \rightarrow \alpha_{171}$) shows peaks at 81.2, 84.2, 102.8, 110.8, and a very weak one at about 126 keV. The region of 92 to 96 keV is congested and has poor statistics. After removing accidentals and the maximum Pa-KX ray intensities, there is still a residue left centering at 92.4 keV. The intensity of this residue relative to the 110.8 keV radiation is roughly the same as found in coincidence with all α particles.

The intensity of the 84.2 keV γ ray per ($\alpha_{304} \rightarrow \alpha_0$) was 6.9 ± 0.4%. After a 4% correction for the α-particle groups which bypass the 84.2 keV state, the intensity of the 84.2 keV γ ray per population to the 84.2 keV state is 7.3 ± 0.4%. Together with the value 6.7 ± 0.5% deduced from the ($\alpha_{113} \rightarrow \alpha_0$) coincidence measurements, the best value for the fraction of the 84.2 keV state which de-excites by an 84.2 keV γ ray is 7.0 ± 0.3%. This is in good agreement with the value 7.2 ± 1.0% found by Asaro et al.[12] for the absolute intensity of this γ ray in $^{231}$Th β decay and confirms their deduction that nearly all of the $^{231}$Th beta decay feeds the 84.2 keV state.

We will now show that the 81.2 keV and 84.2 keV γ rays must be in coincidence with each other, with the 81.2 keV γ ray preceding the 84.2 keV γ ray. The intensity of the 84.2 keV γ ray in coincidence with ($\alpha_{186} \rightarrow \alpha_{171}$) shows that at least 78% of the 183.4 keV level decays through the 84.2 keV state. An 81.2 keV M1 transition has been previously observed[13,14,15] in the decay of $^{231}$Th. If the 81.2 keV γ ray observed in the alpha decay of $^{235}$Np

is the same as that detected in the decay of $^{231}$Th, the intensity of the 81.2 keV transition per ($\alpha_{186} \rightarrow \alpha_{171}$) decay calculated with the theoretical[16] M1 conversion coefficient is 98 ± 13%. Therefore the 81.2 keV transition must be in cascade with the 84.2 keV transition. As there was no 81.2 keV $\gamma$ ray detected in coincidence with ($\alpha_{113} \rightarrow \alpha_0$) (<0.1%), it must precede the 84.2 keV $\gamma$ ray. Either it decays first to a 165.4 keV state from the 183.4 keV level by an 18 keV transition and thence to the 84.2 keV state, or first to a 102.2 keV state and thence to the 84.2 keV state. As there is a $\gamma$ ray of 102.8 keV in coincidence with $\alpha_{186}$ and no detectable 165 keV radiation, the latter possibility seems most likely. Indeed, it will be shown in the $^{231}$Th decay measurements that the 102.8 and 81.2 keV $\gamma$ rays are in coincidence. The KX rays and the possible 165 keV $\gamma$ ray observed in coincidence with all the $\alpha$ particles are not detected in coincidence with $\alpha_{186}$ and are probably in coincidence with $\alpha_{250}$. An upper limit of 0.015% per ($\alpha_{113} \rightarrow \alpha_{84}$) decay can be set from our data on the intensity of any coincident 102 keV $\gamma$ ray. It will be seen from the coincidence work on $^{231}$Th that 3.0 ± 0.4% of the 102.2 keV level decays by a 102.3 keV $\gamma$ ray. Therefore the maximum direct $\alpha$-particle population to the 102.2 keV state is 0.5%, and there must be another close lying state at ≃ 102 keV receiving at least 23% $\alpha$-particle population. The existence of such a state is indicated by previous work[13,14] on $^{231}$Th decay as well as experiments which will be described shortly.

## V. $^{231}$Th γ-RAY SPECTRA

### A. γ-Ray Singles

A γ-ray spectrum taken with the high resolution detector is shown in Fig. 2 and the γ-ray energies and intensities are given in Table III. Also included in this table is data of Holtz[14] from γ-ray and electron spectroscopy measurements. The spectrum was started right after the chemical separation was completed. The sample was placed 5 cm from the detector, and there was no significant external absorber.

The high resolution of the detector enabled us to observe 93.0 and 105.73 keV γ rays which had not been seen before, and this part of the γ-ray spectrum is shown in more detail in Fig. 3. These radiations could not be the $K_{\alpha_1}$ and $K_{\beta_1}$ X rays of Th due to self excitation because there is no detectable Th $K_{\beta_3}$ X ray at 104.8 keV. The maximum contribution of Th KX rays is only 20% of the abundances of either the 93.0 or 105.73 keV γ rays.

The γ rays with energies greater than 200 keV were measured in another experiment with the $^{231}$Th source much closer to the detector and with a 0.006" Pt absorber. Eight spectra were taken for six hours each. The spectra were summed to obtain the best γ-ray energies and abundances. Then the half-lives of nearly all the γ rays above 200 keV were determined from the component 6 hour runs. The best energies and half-lives are given in Table IV.

The assignment of the 240.4, 318.0, and 320.2 keV γ rays to $^{231}$Th is somewhat questionable because they decay with half lives slightly different than 25.5 h, the half-life of $^{231}$Th. However, these three γ rays are so weak that the inaccuracy of the experimental intensities could be responsible for such a disagreement.

γ rays of 308.9 and 311.0 keV were found to decay with the $^{231}$Th half-life. A γ ray of ≃ 310 keV was previously observed by Baranov et al.[15] γ rays from $^{233}$Pa, $^{143}$Ce, and $^{140}$La observed in our spectrum, indicate that these elements were not completely separated in the chemical purification of the source. All γ-ray energies in our singles measurements were relative to the value of 84.17 keV for the 84 keV γ ray. This value has been previously obtained from high resolution electron spectroscopy measurements by Hollander et al.[13]

## B. γ-γ Coincidence Measurements

These measurements were made with a multidimensional analyzing system described earlier. The γ-ray analysis was started after the conclusion of the chemistry and lasted for 2 days. We have only included in this paper the results from those computer runs which were the most fruitful. The γ-ray gate energies and the coincident γ-ray energies and abundances are tabulated in Table V, while the coincidence spectra are shwon in Figs. 4 and 5.

### 1. $\gamma_{84}$-γ Coincidences

A very intense γ ray of 81.1 keV is observed, and, as discussed under $^{235}$Np α decay, it must decay almost entirely through the 84.2 keV level. The intensity ratios between the 81.1 keV γ ray and all of the others (except the 63.7 keV γ ray) are about the same in this coincidence spectrum and in the singles spectrum. Therefore, these γ rays must also decay almost entirely through the 84.2 keV state. The 63.7 keV γ ray was obscured by Compton radiation in the singles spectrum but may also decay almost entirely through the 84.2 keV state. The γ rays of 81.1, 82.1, and 99.4 keV are assumed to decay from a

183.47 keV level and populate states at 102.30, 101.38, and 84.17 keV respectively. A 183.47 keV γ ray which is observed in the singles γ-ray spectrum, is probably the "cross over" transition. γ rays of 163.1 and 146.0 keV determine a level at 247.33 keV[14] which decays to the 183.47 keV state by the 63.7 keV γ ray observed in this coincidence spectrum. γ rays of 89.9, 72.5 keV, and 174.11 keV are assumed to decay from a 174.10 keV level. As the 174.11 keV γ ray was not observed in coincidence with $^{235}$Np $\alpha_{186}$, it does not de-excite the 183.47 keV level to the 9.3 keV state to an appreciable extent. γ rays of 134.1 and 116.9 keV are assumed to de-excite a 218.28 keV state and populate levels at 84.17 and 101.38 keV. A level at 111.62 keV is indicated by the 106.6 and 135.7 keV γ rays which decay from the 218.28 and 247.33 keV states respectively. Finally, the 218.0 and 236.3 keV γ rays are assumed to de-excite a 320.3 keV level and populate the 102.30 and 84.17 keV states respectively. All the energy levels determined from this measurement, except the ones at 218.2 and 111.62 keV, had been previously found by Holtz.[14]

2. $\gamma_{163}$-γ Coincidences

The purpose of this measurement was to calibrate the efficiency of the system with the 84.2 keV γ ray. The 163.16 keV γ ray de-excites directly to the 84.17 keV state, and the intensity of the 84.17 keV γ ray is known from $^{235}$Np alpha decay to be 7.0% of the events populating the state. The 163.16 keV γ ray was chosen as a gate in this measurement because the Compton background under the peak is relatively low.

3. $\gamma_{218}$-γ Coincidences

The spectrum in coincidence with a 225 keV gate of the same width as the 218 keV gate was measured to estimate the coincidences due to the Compton

continuum under the 218 keV $\gamma$ ray, and the values in Table V have been corrected for this effect. The 218.00 keV $\gamma$ ray populates the 102.30 keV state which de-excites predominantly through the 84.17 keV state, rather weakly to the ground state via the 102.1 keV $\gamma$ ray and very weakly to an excited state at 9.3 keV via the 93.3 keV $\gamma$ ray.

Holtz[14] assigned an E1 multipolarity to the 102.1 keV $\gamma$ ray from his conversion electron spectra. As he did not observe the conversion electrons of the 93.3 keV $\gamma$ ray, their intensity may well be smaller than those of the 102.3 keV $\gamma$ ray which he did see. With Holtz's value of 0.17 for the L conversion coefficient of the 102.3 keV transition and the relative intensities of the 93.3 keV and 102.1 keV $\gamma$ rays from our coincidence and singles measurements, the L conversion coefficient of the 93.3 keV transition is then <2. The theoretical M1, E1, and E2 conversion coefficients[16] are 4.1, 0.11, and 12.8 respectively, so the 93.3 keV transition probably has E1 multipolarity.

## 4. $(\gamma_{81} + \gamma_{82}) - \gamma$ Coincidences

Nearly 30% of the gate spectrum was due to the 84.2 keV $\gamma$ ray, and this made the determination of intensities and the detection of the 93 keV $\gamma$ ray difficult. Another coincidence measurement was made in which the (81 + 82) keV gate contained much less 84.2 keV $\gamma$ ray, and this spectrum is shown in Fig. 4c.

The 81.2 keV $\gamma$ ray populates the 102.30 keV state which gives rise to the 84.2, 102.4, and 93.1 keV $\gamma$ rays as discussed under 218 keV $\gamma$-$\gamma$ coincidences. The 82.1 keV $\gamma$ ray populates the 101.38 keV state which de-excites to the 84.17 keV level. We can show from the coincident abundance of the 63.7 keV $\gamma$ ray, that it is in complete coincidence with both the 84.2 keV $\gamma$ ray and

the composite (81 + 82) keV radiation. The 183.47 keV level feeds the 84.17 keV level by 81.2, 82.0, and 99.3 keV $\gamma$ rays as indicated earlier. These $\gamma$ rays have an effective average conversion coefficient of 8,[14] and their total transition intensity is 17% of the abundance of the 84.2 keV $\gamma$ ray. If the abundance of the 63.7 keV $\gamma$ ray observed in coincidence with $\gamma_{84}$ (0.048 ± 0.016%) is divided by 17%, the value 0.28 ± 0.10% is obtained. This should be the abundance of the 63.7 keV $\gamma$ ray per composite ($\gamma_{81}$ + $\gamma_{82}$) gate if it completely precedes these transitions, and it is indeed in good agreement with the measured value 0.30 ± 0.06%. Therefore we assume the 63.7 keV $\gamma$ ray populates the 183.47 keV state from a 247.33 keV level. Conversion electrons of this transition have been previously observed,[13,14,15] and it has been assigned a predominantly M1 multipolarity.

A $\gamma$ ray at 136.4 keV is appreciably more intense and different in energy from the 135.7 keV $\gamma$ ray which is in coincidence with the 84 keV radiation. Although it could arise in part from backscatter of the 218 keV $\gamma$ ray, a comparison of the spectrum in coincidence with ≈ 76 keV radiation, indicated less than 20% of the residual 136.4 keV radiation could be due to this effect. This $\gamma$ ray de-excites from a state at 320.31 keV to that at 183.47 keV. By similar reasoning to that given for the 63.7 keV $\gamma$ ray, it can be shown that the coincidence intensity is consistent with the singles intensity for the 136.4 keV $\gamma$ ray.

5. $\gamma_{90}$-$\gamma$ Coincidences

The 89.9 keV $\gamma$ ray de-excites from the 174.10 keV state to the 84.17 keV level. The 44.11 keV $\gamma$ ray is assumed to be the rotational transition from the

218.28 keV level to that at 174.10 keV. The 73.0 keV $\gamma$ ray observed in this spectrum was first thought to be due to coincidences between the 72.7 keV $\gamma$ ray and the Compton tails of other $\gamma$ rays. However, this $\gamma$ ray was not seen in coincidence with a gate composed mainly of the Pa $K_{\alpha_2}$-X ray at 92 keV and therefore is not a spurious effect. The 73.0 keV $\gamma$ ray was placed in the decay scheme as a transition from the 247.33 keV state to the 174.10 keV level. This was confirmed by measuring the $\gamma$-ray spectrum in coincidence with $\gamma_{72.7}$.

6. $\gamma_{72.7}$-$\gamma$ Coincidences

The gate contained a large contribution of Compton tails from other $\gamma$ rays. In order to correct for this effect, the spectrum in coincidence with a gate at about 76 keV was measured.

The 73.0 and 72.7 keV $\gamma$ rays were detected in one unresolved peak in both detectors in the coincidence measurements, therefore the intensity of $\gamma_{73}$ per 100 $\gamma_{72.7}$ events obtained from the coincidence spectrum is twice the real intensity. The actual intensity of this $\gamma$ ray is consequently 0.36 ± 0.06% which is about the same as found in coincidence with $\gamma_{90}$ (0.40 ± 0.16%). We conclude therefore that the 73.0 keV $\gamma$ ray definitely de-excites through the 174.10 keV state.

The intensity of $\gamma_{84}$ in this coincidence measurement shows that 93 ± 12% of the 101.38 keV state decays through the 84.17 keV level.

7. $\gamma_{102}$-$\gamma$ Coincidences

The 81.2 keV $\gamma$ ray was observed in the coincidence spectrum and the 82.1 keV $\gamma$ ray was not, which is consistent with the former populating the 102.30 keV state and the latter populating the 101.38 level.

The 135.7 kev γ ray, which we assume de-excites from the 247.33 keV state to the 111.62 keV level, was not observed in this measurement and a limit of 0.015% could be placed on its abundance. Consequently less than 2.5% of the 111.62 keV level de-excites through the 102.30 keV state. As the ratio of the intensities between the 81.2 and 218.0 keV γ-rays in this coincidence experiment is the same as in the singles measurement, all of the latter γ ray must de-excite through the 102.30 keV level. The abundance of the 145.2 keV coincident γ ray corresponds to 75 ± 30% of the singles intensity and therefore is consistent with all of the singles γ-ray intensity populating the 102.30 keV state. It is tempting to assume that the 145.2 keV γ ray is an E2 transition between the 247.33 and 102.30 keV states. No conversion lines of the 145.2 keV transition were observed, however, in the appropriate intensity by either Hollander et al.[13] or Holtz[14] even though those of the 146.0 keV γ ray were seen. Therefore the 145.2 keV γ ray may possibly be an E1 transition. The 137.0 keV γ ray observed in this coincidence measurement has an intensity consistent with that of the singles measurement.

## VI. $^{235}$Np ALPHA DECAY SCHEME

An alpha decay scheme based on our work and previous results[10,13,14] is shown in Fig. 6.

The ground state of $^{231}$Pa has a measured spin[17] of 3/2 and it has been interpreted by Stephens et al.[18] as the I = 3/2 member of an odd parity K = 1/2 rotational band.

A 58.5 keV level was found to be populated by Coulomb excitation of $^{231}$Pa,[19] in the beta decay of $^{231}$Th[13,14,15] and in the electron capture of $^{231}$U.[13] A highly converted 58.5 keV $\gamma$ ray which de-excites this level has been observed in the present work. There was no attempt, however, to detect the 25 keV $\gamma$ ray previously observed by Gindler et al.,[10] which populates the 58.5 keV level through the 84.2 keV state. The 58.5 keV state has been interpreted by Hollander et al.[13] as the I = 7/2 member of the 1/2 - (530) ground state rotational band.

The state at about 8 keV populated by $\alpha_8$ is probably the I = 1/2 member of the ground state rotational band. A more accurate energy for this state, 9.3 keV, is obtained from the beta decay of $^{231}$Th.

From $^{231}$Th beta decay the I = 5/2 member of the ground state rotational band was found at 77.8 keV. $\alpha$-particle population to this state was not observed but it could easily be masked by the very intense $\alpha$-particle group which populates the 84.2 keV state.

The 84.2 keV state receives the most intense $\alpha$-particle population and it has been previously[10,13] assigned as the spin 5/2 member of the 5/2 + (642) Nilsson orbital. This assignment was consistent with the existence of a favored alpha transition to this level with a hindrance factor of 3.3.[10] We found in this work, however, that both the 84.2 and 183.4 keV states are populated by apparently favored $\alpha$-particle groups with about the same low hindrance factors (4.3).

The 102.2 keV state is not directly populated by α particle emission but receives population through the 183.4 keV level by means of the 81.2 keV transition. The 102.2 keV level decays almost entirely to the 84.2 keV state, but a small fraction goes directly to the ground state by a 102.2 keV γ ray. This γ ray was previously observed in the beta decay of $^{231}$Th by Hollander et al.[13] and by Holtz,[14] who assigned an E1 multipolarity to it and an even parity to the 102.2 keV state. From our measurements on $^{231}$Th decay we have assigned a spin 3/2 and the Nilsson orbital 3/2 + (651) to this level. There is no detectable α-particle population to the 102.2 keV state but there is another close-lying state at 103 ± 4 keV which receives at least 23% of the α-particle population of $^{235}$Np. This latter state is very likely the same as that at 101.38 keV found in $^{231}$Th decay. It is probably the I = 7/2 member of the 3/2 + (651) rotational band, and the states at 84.2, 113, and 169.3 keV are the I = 5/2, 9/2, and probably 11/2 members respectively of the same rotational band. The best energy for the 113 keV state is 111.62 keV from $^{231}$Th decay. A 110.8 keV radiation was observed in coincidence with all α particles and with α-particle gates in the region of $\alpha_{186} \rightarrow \alpha_{171}$. We believe this γ ray is the transition between the 11/2 and 9/2 members of the ground state rotational band. The best energy of the I = 11/2 state, 169.3 keV, is in good agreement with the energy obtained from the α-particle spectrum.

A ∿ 185 keV γ ray was observed in coincidence with the total $^{235}$Np α spectrum and also with $\alpha_{186}$. This is probably the same as the 183.4 keV γ ray detected in $^{231}$Th decay, which defines a state at that energy. This state must decay preominantly through the 84.2 keV state as shown from the $^{235}$Np α-γ coincidence measurements, and is very likely the band head of the 5/2 + (642) favored rotational band. The assignment is consistent with the low hindrance factor (4.4) of the α-particle group which populates this level. States at

250 and 304 keV populated by α-particle groups with relatively low hindrance factors are very likely the I = 7/2 and 9/2 members of the same rotational band. A strong Coriolis coupling of this band with the 3/2 + (651) introduces large admixtures of the favored band in the states at 84.2, 103 ± 4 and 113 keV, leading to an intense α-particle population. The I = 3/2 state at 102.2 keV is not mixed with the favored state and consequently does not receive appreciable α-particle population ($\leqslant 0.5\%$).

The energy spacing and the inversion of the I = 3/2, 5/2, and 7/2 levels in the K = 3/2 rotational band is also a consequence of the Coriolis interaction with the even parity rotational bands, as it will be shown later. This interpretation has been previously suggested by Hoekstra and Wapstra[2] based on the similarity with the energy levels in $^{233}$Pa.[1,2]

## VII. $^{231}$Th DECAY SCHEME

The decay scheme of $^{231}$Th has been previously studied by Baranov et al.,[15] Hollander et al.,[13] Asaro et al.,[12] and lately by Holtz.[14]

Most of the decay of $^{231}$Th populates the level at 84.17 keV directly or through intermediate states. This state de-excites to the ground state rotational band,[13,14] by means of 84.17 and 25.65 keV E1 transitions.

The 102.30 keV state decays to the ground state and to a 9.3 keV level by E1 $\gamma$ rays of 102.30 and 93.3 keV respectively. As the parity of the ground state is odd, the parity of the 102.30 keV state is therefore even, and that of the 9.3 keV level is odd. If we assume that this latter state is the I = 1/2 member of the ground state rotational band, spins of 1/2 and 3/2 are possible for the 102.30 keV level.

The 101.38 keV state decays to the I = 7/2 member of the ground state rotational band at 58.47 keV by a 42.80 keV E1[14] transition and hence has even parity. As a possible 101.4 keV $\gamma$ ray from the decay of this level to the ground state was not observed, the spin of the 101.38 keV state is either 7/2 or 9/2.

The 183.47 keV state populates both the 101.38 keV and the 102.30 keV states by M1 $\gamma$ rays, and therefore it must have a spin of 5/2 and even parity. Consequently the 102.30 and 101.38 keV levels have spins of 7/2 and 3/2 respectively. We found from our $\gamma$-$\gamma$ coincidence measurements that these two states de-excite to the 84.17 keV level. The conversion electrons of the corresponding 18.07 and 17.21 keV transitions were observed by Hollander et al.[13] The decay patterns of the 84.17, 101.38, and 102.30 keV state are consistent with the expectations for a K = 3/2 rotational band if the 102.30 keV state is the band head, and the I = 5/2 and 7/2 members are at 84.17 and 101.38 keV

respectively. We assigned the Nilsson orbital 3/2 + (651) to this rotational band, and the orbital 5/2 + (642) to the spin 5/2 state at 183.47 keV.

The state at 247.33 keV is de-excited by M1[14] γ rays of 146.00 and 163.16 keV which populate levels at 101.38 keV and 84.17 keV respectively, and by a 135.77 keV γ ray which populates the 111.62 keV state. If we assume that this latter state is the I = 9/2 member of the 3/2 + (651) rotational band, then the 247.33 keV state must have even parity and a spin of 7/2. From the alpha decay of $^{235}$Np we have interpreted this state as the I = 7/2 member of the 5/2 + (642) rotational band.

The anomalous order and spacing of the levels at 84.17, 101.38, and 102.30 keV as well as the large energy separation between the I = 5/2 and 7/2 states at 183.38 keV and 247.33 keV are due to the Coriolis mixing of the even parity rotational bands as will be explained in detail in Sec. IX.

A 174.10 keV odd parity state, defined by an E1[14] γ ray of 89.94 keV which populates the 84.17 keV state, has been previously observed by other authors.[13,14] This state also decays to the ground state by a 174.19 keV γ ray.

A new odd parity state was observed at 218.28 keV. This state is de-excited by an E1 γ ray[14] of 116.91 keV which populates the 101.38 keV level, and by γ rays of 134.14 and 106.58 keV which populate the 84.17 keV and 111.62 keV states respectively. The states at 174.10 keV and 218.28 keV are probably the band head and the I = 7/2 member respectively of the 5/2 - (523) rotational band. This assignment is consistent with the energy spacing between the two states, 44.2 keV. This agrees well with values found for the same orbital[20] in $^{235}$Np (42.6 keV),[21] $^{237}$Np (43.4 keV),[22] and $^{239}$Np (43.1 keV).[23,24]

States at 320.31 keV and 351.97 keV observed before by Holtz[14] have been seen also in this work. Unfortunately the experimental data available is not sufficient to make any definite assignment. The decay pattern of these levels, however, suggest that they have spins of 3/2 and 5/2 respectively.

$\gamma$ rays of 240.4, 242.6, 169.58, and 105.73 keV which respectively de-excite states at 318.2, 320.31, 247.33, and 183.47 keV, define a level at 77.8 keV. This latter state is very likely the I = 5/2 member of the ground state rotational band which had been previously placed at 76.04 keV by Hollander et al.[13]

A decay scheme based on this work and previous results[13,14] is shown in Fig. 7.

## VIII. $^{231}$Th BETA POPULATIONS AND TRANSITION INTENSITY BALANCES

The beta population to the various states which are deduced in this section and the γ-ray energies and total transition abundances which populate and depopulate these states are shown in Table VI. Where no explanation is given, the γ ray energies, abundances and multipolarities from Table III were used along with theoretical conversion coefficients.[16] The multipolarities of the observed γ rays with energies between 218 and 320 keV are probably either E1 or M1. As a rule these have a negligible effect in the transition intensity balance and we have used average values for the E1 and M1 theoretical conversion coefficients[16] to calculate the transition intensities.

Ground state. It has been previously reported that essentially all of the beta decay processes go through the 84 keV level.[12] Although our measurements alone can be used to deduce relative beta intensities to the levels in $^{231}$Pa from 84 keV and higher, they shed very little light on the beta populations to the low lying states. If we combine our value of the fraction of the 84.17 keV level which de-excites by the 84.17 keV photon, 7.0 ± 0.3%, and the value found by Asaro *et al.*[12] for the intensity of the 84 keV photon per beta decay, 7.2 ± 1%, we can obtain limits on the beta populations to the low lying states in $^{231}$Pa. The abundance of the beta transitions which bypass the 84.17 keV state is then -3 ± 14% or < 11% of those transitions which eventually feed the 84.17 keV level. From the decay scheme, the γ transitions which bypass the 84.17 keV state amount to ∿ 1%. Therefore the total beta population to the ground and first three excited states should be less than 10% of the betas which feed the 84.17 keV level.

9.3 keV state. The beta population must be less than 10% to this level as discussed above. The 68.5 keV transition populating this state has only been observed[13,14,15] by its conversion electrons. The relative intensity (0.6%) of the conversion electrons of this transition to those of the 58.5 keV transition was taken from Hollander et al.[13] The depopulation of this state is 0.5% plus any direct beta population, and therefore is less than 10%. The 9.3 keV transition has not been detected yet.

58.47 keV state. As given earlier in the ground state section, the beta population to this state is less than 10%. There are two other ways of determining this abundance. From the coincidence measurements with the 72.66, 81.18, 89.94, and 163.16 keV $\gamma$ rays as gates the average ratio between the abundances of the 58.3 and 84.2 keV $\gamma$ rays was 7.7 ± 1.0%. Any direct beta population to the 58.47 keV level or transition populations which bypass the 84.17 keV state will cause this ratio to be larger in the singles measurement. From the singles value of 7.2 ± 0.7%, the beta population feeding the 58.47 keV state while bypassing the 84.17 keV level is -7 ± 17% of the decay to the 58.47 keV state. As the 58.47 keV transition represents 80% of the total decay, the maximum abundance of direct beta decay to the 58.47 keV state is 8% for two standard deviations.

A third way of determining the maximum beta abundance is from the transition intensity balance. The total transition intensity out of the state is 79%. The major input transition is the 25.65 keV transition. Although this transition probably has a small anomaly[12] in its $L_I$, $L_{II}$, $M_I$, and $M_{II}$ conversion coefficients, the ratios of total L to $L_{III}$[25] and total M to $M_{III}$[13,25] conversion coefficients are only about 3% smaller than the theoretical values.[26]

We assume a conversion coefficient of 4.18 which is 97% of the theoretical value for the 25.65 keV transition. The difference between the 25.65 and 58.47 keV transition intensities is 6.9 ± 9% or < 16% for two standard deviations. This limitation applies to the sum of any direct beta decay and also population of the 77.8 keV state followed by de-excitation of a 19.3 keV transition.

Baranov[15] has reported electrons of a 19.8 keV transition but did not give any intensity information. Hollander et al.[13] found unassigned lines which could correspond to $M_I$, $O_I$, and $N_I$ conversion electrons of a 19.14 keV transition in $^{231}$Th decay, but did not observe these lines in $^{231}$U decay in a weaker exposure. The abundance of this transition is > 0.5% if the $M_I$ line is correctly assigned, and > 4.5% if the $O_I$ is correctly assigned. The upper limit comes from the intensity balance and is < 16% just as discussed in the preceding paragraph.

77.8 keV state. The direct beta population is less than 10% as given earlier in the ground state section. From the intensity balance, the unobserved 6.4 keV transition should have an intensity of < 17%, but a better limit will be obtained below.

84.17 keV state. From our value of the 84.17 keV γ-ray intensity, 7.0 ± 0.3%, per population to the 84.17 keV level; the conversion coefficient of the 84.17 keV γ ray, 2.8, previously measured;[12] our ratio between the intensities of the 84.17 and 25.65 keV γ rays, and the conversion coefficient of 4.18 for the 25.65 keV γ ray discussed earlier; 100 ± 11% of the 84.17 keV state decays by 84.17 and 25.65 keV transitions. No 6.4 keV transition to the 77.8 keV state has been observed, and from the intensity balance its

abundance is < 11%. The abundance of the 17.21 and 18.13 keV transitions will be discussed under the 101.38 and 102.30 keV levels respectively. The beta population to the 84.17 keV level from the intensity balance is ∿ 63%, with a large error reflecting the uncertainty in the abundance of the 17.21 keV transition.

101.38 keV state. The beta population to this level can be crudely determined from the abundance of the 42.6 keV γ ray in coincidence with the 82.02 keV transition. This calculated beta population, 11%, is only approximate because of the large statistical error in the coincidence measurement. For ± one standard deviation, the calculated beta population varies from 5% to 27%. The abundance of a possible 0.9 keV transition from the 102.30 keV level will be discussed in that section. The 17.21 keV transition has an abundance of 17% from the intensity balance, but with a large uncertainty reflecting that in the beta population.

102.30 keV state. The abundance of the 102.30 keV γ ray in the 218 keV γ-γ coincidence experiment was 3.0 ± 0.4%. This value together with the singles intensity leads to a total population of 15 ± 3%. The abundance of the γ transitions feeding this level is 9.3% which leaves a beta population of 6 ± 3%. The abundance of the 18.13 plus 0.9 keV transitions is then 15 ± 3% as the other γ-ray transitions de-exciting the level have small intensities. The maximum abundance of the 0.9 keV transition may be inferred from the work of Hollander et al.[13] who observed electrons of the 17.21 keV transition prominently in $^{231}$Th decay but not in $^{231}$U decay, although the 18.13 keV transition was even more prominent in the latter case. As the O lines of the 18.13 keV transition were observed and the M lines of the 17.21 keV transitions were not seen, we assume the 0.9 keV transition to be less than 10% of the total, or < 1.5%. No electrons of the 0.9 keV transition have yet been observed.

174.10 keV state. The intensity of the 44 keV $\gamma$ ray will be discussed under the 218 keV level. The intensity of the direct beta decay which populates this state is obtained from the intensity balance of the transitions, and the error reflects that in the 44 keV transition.

183.47 keV state. The intensity of the 63.8 keV transition will be discussed under the 247.33 keV level. The abundance of the beta decay to this level is determined from the transition intensity balance. The error reflects the uncertainty in the $\gamma$-ray singles intensities.

218.22 keV state. The abundance of the 44 keV $\gamma$ ray in coincidence with the 89.94 keV $\gamma$ ray was $0.24 \pm 0.16\%$. This is presumably an M1 + E2 rotational transition. We have used a conversion coefficient of $(100 \pm 30)$ which assumes the transition to be predominantly M1 with an M1-E2 mixing ratio for electrons equal to that found for the 63.8 keV rotational transition by Holtz.[14] The abundance of the 44 keV transition is then $0.40 \pm 0.4\%$. The beta abundance to this level was obtained from the transition intensity balance and the error reflects the uncertainty in the intensity of the 44 keV transition.

247.33 keV state. The abundance of the 63.7 keV $\gamma$ ray in coincidence with the $(81.18 \pm 82.02)$ keV $\gamma$ rays was $0.30 \pm 0.06\%$. From the relative L subshell intensities of Holtz for this M1 + E2 transition and theoretical conversion coefficients[16] we calculated a conversion coefficient of 19. The abundance of the 63.7 keV transition is then $0.94 \pm 0.18\%$. The beta abundance to this level was obtained from the transition intensity balance. The error reflects the uncertainty in the $\gamma$-ray singles measurement.

## IX. CORIOLIS EFFECTS

In S. G. Nilsson's[27] treatment of single particle states in deformed nuclei, two interactions, which sometimes are prominent, were not included. One of them, the Coriolis interaction, was treated initially by Kerman[28] in his study of the energy levels of $^{183}W$ and has been observed extensively in heavy nuclei. The other involves an interaction between states whose principal quantum numbers differ by 2 and has also been observed but less often.

The Coriolis interaction occurs between states with the same spin and parity but whose K quantum numbers differ by ±1. The magnitude of the interaction depends on the strength of the interaction matrix element and the energy spacing of the interacting states. The effect of the interaction is to alter the energies of the levels, and to introduce impurities in the wave function. This latter effect will influence $\alpha$, $\beta$, and $\gamma$ transition probabilities.

a. Energy Levels. A Coriolis calculation was made of the expected energies of the observed even parity states considering the interaction between the 1/2 + (651), 3/2 + (651), 5/2 + (642), 7/2 + (633) and 9/2 + (624) orbitals. The secular equations for each spin were solved by using a computer program BETABLE written by Thomas P. Clements of this laboratory. This program solved the secular determinants for all the spin values involved, simultaneously adjusting all the parameters until a least squares fit to the experimental energy levels was made. The program also gives the admixtures in the wave functions for the final fit.

The energies of the unperturbed quasi-particle states were obtained with the following equation:[29]

$$E_i = \sqrt{(\varepsilon_i - \lambda)^2 + \Delta^2} \qquad (1)$$

where $\varepsilon_i$ are the Nilsson single particle energies,[27] $2\Delta$ is the even-even energy gap and $\lambda$ is the energy of the Fermi surface. We used interpolated Nilsson eigenvalues $\varepsilon_i$ for a deformation of $\delta = 0.23$ and a value of 0.63 for $\Delta$. The energy of the Fermi surface was selected as 100 keV above the ground state energy to obtain 30 keV between the 3/2 + (651) and 5/2 + (642) orbitals. This gave a Coriolis interaction between these orbitals strong enough to invert the spin 3/2, 5/2, and 7/2 members of the 3/2 + (651) rotational band.

The 1/2 + (660) orbital was predicted to be 200 keV above the 3/2 + (651). We used, however, in our calculations a value of 400 keV since we should have detected the state if it were as low in energy as 200 keV.

Once the calculation was performed, the program normalized the final perturbed energies for the best fit to the lowest energy state, which in this case was the 84.17 keV level. We fit the 101.38, 102.30, 111.62, 183.47, and 247.33 keV states using the following variable parameters:

$h^2/2\mathfrak{J}$, the rotational constant;

$a_{1/2}$, the decoupling constant of the 1/2 + (660) rotational band;

$A_{1/2,3/2}$, the Coriolis matrix element between the 1/2 + (660) and 3/2 + (651) orbitals;

$A_{3/2,5/2}$, the Coriolis matrix element between the 3/2 + (651) and 5/2 + (642) orbitals;

$E_{5/2}$, energy of the unperturbed 5/2 + (642) orbital.

With five unknown energies and five variables, the calculation of course gave exact agreement. The fitted values of the parameters, however, were reasonable when compared to theoretical expectations as shown in Table VII. The theoretical Coriolis matrix elements used here were calculated from Nilsson type wave functions by Bunker and Reich.[30] The reduction in the fitted values for

$A_{3/2,5/2}$ and $A_{1/2,3/2}$ are not unusual as reduction factors of up to 2 or 3, possibly due to pairing correlations, are normally found for interactions between states near the Fermi surface.[31,32]

The value 3.7 for the decoupling parameter of the 1/2 + (660) rotational band is smaller than the theoretical value 6.5, but similar to the experimental value of 4.5 reported by Borggreen et al.[33] for the same orbital in $^{159}$Gd.

It should be noted that this set of final values of the parameters is not unique, that is, the same energy levels can be reproduced using different set of values for the parameters which were not varied in the calculation. This set, however, is the best that can be obtained with the present experimental data and should be adequate for calculation of α, β, and γ transition probabilities. In Table VIII are tabulated the calculated admixtures of the various Nilsson orbitals in the wave functions of the states just discussed.

b. Gamma-Ray Transition Probabilities. Electromagnetic transition rates in $^{231}$Pa are expected to be influenced by the strong Coriolis coupling between the even parity rotational bands.

We have calculated the reduced transition probability of the M1 γ rays which de-excite the 183.47 and 247.33 keV states taking into account the effect of the Coriolis mixing of the rotational bands. In this case, the M1 reduced transition probability is given by:

$$B(M1, I \rightarrow I') = \frac{3}{16\pi}\left(\frac{e\hbar}{2Mc}\right)^2 \Bigg| \sum_{KK'} a_K\, b_{K'}\, [\langle I\ 1\ K\ K'-K | I\ 1\ I'K' \rangle$$

$$\times\, GM1(K \rightarrow K') + (-1)^{I'+K'} \times \langle I\ 1\ K - K'-K | I\ 1\ I'-K' \rangle \times GM1(K \rightarrow -K')]$$

$$\times\, (U_K\, U_{K'} + V_K\, V_{K'})\Bigg|^2$$

where $a_K$ and $b_{K'}$ are the admixtures in the wave functions of the upper and lower states respectively and they are given in Table VIII; GM1($K \rightarrow \pm K'$) are the $\gamma$-transition single particle matrix elements,[27] $U_K$ and $V_{K'}$ the pairing coefficients,[29] and the quantities in brackets are Clebsch-Gordon coefficients.

The matrix elements GM1($K \rightarrow \pm K'$) were calculated with the formulas given in Ref. 27 using the gyromagnetic factors $g_\ell = 1$, $g_R = Z/A = 0.39$ and $g_S = 0.6\ g_{S.free} = 3.35$. The Nilsson coefficients $a_{1\Lambda}$ in the uncoupled basis were obtained from those given by Davidson[34] for proton states in the coupled representation ($C_{j\Omega}$).

The pairing factors ($U_K U_{K'} + V_K V_{K'}$) are all equal to unity except those which correspond to the K = 1/2 and 3/2 rotational bands, i.e. ($U_{1/2}U_{3/2} + V_{1/2}V_{3/2}$) and ($U_{3/2}U_{5/2} + V_{3/2}V_{5/2}$). As the correction of the Coriolis matrix elements for the pairing correlation effect is the same as for M1 transition probabilities,[29] the pairing factors mentioned above are given by the ratio between the Coriolis matrix elements used in the best fit and the theoretical values. These factors are respectively 0.73 and 0.38.

Our calculated branching ratios considering both pure (column 3) and mixed (column 4) rotational bands are compared with the experimental results in Table IX. The E2 component of the 99.30 keV $\gamma$ ray was found to be $\sim$ 65% from the $L_I/L_{III}$ subshell ratio given in Ref. 14, and this component was removed from the experimental branching ratio. The calculation was performed with a computer program MIXING.[35]

The four experimental ratios shown in Table IX agree much better with the theoretical values deduced from the mixed wave functions than with the Clebsch-Gordan coefficient ratios (pure wave functions). The discrepancy of a factor of 4 between theory and experiment for the ratio of $B_{135.7}/B_{163}$, however, indicates the need for further improvement in the wave functions.

c. Alpha-Particle Transition Probabilities. The ground state alpha decay reduced transition probabilities for nuclides with even number of neutrons and protons follow closely to theoretical expectations and are normally described as unhindered alpha decay.[36] Although odd mass alpha emitters often have alpha transition probabilities which are highly hindered, in those cases where the parent and daughter states have the same single particle configuration this hindrance is usually about a factor of only 1 or 2. These transitions are called favored. In some nuclei other states may interact strongly with the favored levels and hence contain admixtures of them and likewise receive a substantial alpha population.

$^{235}$Np α decay demonstrates this type of interaction as the alpha populations to the 84.17 and 183.47 keV states each have a low hindrance factor of about 4.3. These states interact strongly by the Coriolis interaction and have rather impure wave functions. We have used an equation similar to that used by Pilger, et al.[37] in the α decay of $^{235}$U to calculate the expected hindrance factors:

$$\frac{1}{HF} = \frac{1}{N} \sum_{L=0,2,4} \left( \sum_{K=3/2,5/2} \frac{a_{KI_i}\, a_{KI_f} \langle I_i\ L\ K\ 0 | I_i\ L\ I_f\ K_f \rangle}{HF_{L(e-e)}} \right)^2, \quad (3)$$

where HF is the hindrance factor for the α decay to states strongly perturbed by the Coriolis interaction, N is a factor generally between 1 and 2 which expresses the hindrance of the favored transition over the even-even value, $a_{Ki}$ are the admixtures of K = 3/2 and K = 5/2 in the parent and daughter states, $HF_{L(e-e)}$ are the hindrance factors from the adjacent even-even nuclei for L = 0, 2, 4 alpha waves with respective values of 1.0, 1.18, and 35, and the quantity in brackets is a Clebsch Gordan coefficient.

Although this equation ignores unfavored decay between states of different Nilsson configuration, the only transition of concern here is that between the K = 3/2 and K = 5/2 rotational bands. Poggenburg[38] has shown that is expected to be hindered by about a factor of 400 so it would only be of major concern in the alpha population to the spin 3/2 state at 102.30 keV.

The values for the admixtures in the daughter nucleus were taken from Table VIII. As the parent admixture of K = 3/2 is unknown, we calculated abundances using admixtures of 0.1 and 0.2 of K = 3/2 respectively in the parent nucleus. The calculated and experimental hindrance factors are shown in Table X.

The agreement here is about as good as one generally obtains in a Coriolis calculation[37] of α-decay probabilities. The failure of an exact quantitative agreement probably lies not only in the uncertainties in the Coriolis admixtures in the parent nucleus and the neglect of the less prominent intrinsic decays but in a partial failure[38] of the Bohr, Froman, and Mottelson model.[36]

d. Beta-Decay Transition Probabilities. In Table X are shown the experimental ft values for the even parity states in $^{231}$Pa populated in the β decay of $^{231}$Th, and the relative values calculated with pure and Coriolis-mixed wave functions. The equations used for the calculations were, respectively:

$$\frac{1}{ft} \propto G^2_{K_i K_f} \langle 5/2\ 1\ K_f\ K_f - K_i | 5/2\ 1\ I_f\ K_f \rangle^2$$

and

$$\frac{1}{ft} \propto \left| \sum_{K_f=3/2, I_f} a_{K_f}\ G_{K_i K_f}\ U_{K_f} \langle 5/2\ 1\ K_f\ K_f - K_i | 5/2\ 1\ I_f\ K_f \rangle \right|^2 , \quad (4)$$

f is the integrated Fermi function, t is the partial β-decay half-life $K_i$ for the $^{231}Th$ ground state is 5/2, $G_{K_iK_f}$ are proportional to the β-decay matrix elements between the states $K_i$ and $K_f$, $U_{K_f}$ are the pairing coefficients for the final states, $a_{K_f}$ are the Coriolis admixtures taken from Table VIII, and the other quantities are described in part a) of this section.

We considered the Fermi interaction to be negligible[39], and for pure Gamow-Teller allowed transitions the $G_{K_iK_f}$ could then be calculated from Nilsson equations[27] for M1 electromagnetic transition probabilities. The calculated values for $G_{3/2,3/2}$, $G_{3/2,5/2}$, and $G_{5/2,7/2}$ are 0.307, 0.721, and 1.05 respectively. The values of $U_{3/2}$ and $U_{5/2}$ are 0.57 and 0.98 respectively and are determined from the ratios of the experimental ft values to the 102.3 and 183.4 keV states together with the pairing factor 0.38, discussed in Sec. IX.b. $U_{7/2}$ was taken as unity for the K = 7/2 particle state which lies far from the Fermi surface.

The beta population to the 102.30 keV state, which is not Coriolis-admixed with higher K values, agrees well with the value calculated with pure wave functions; while the populations to the 101.38 and 84.17 keV states, which are strongly Coriolis-admixed with higher K values, are much higher. The agreement is much better with the Coriolis-mixed wave functions which include pairing correlation. The discrepancies in the values for the 84.17 and 101.38 keV states may be due in part to the experimental uncertainty in the way the 74% beta population to these two states is divided.

## X. CONCLUSIONS AND SUGGESTIONS

1. Nilsson level assignments have been made for three low lying rotational bands in $^{231}$Pa in addition to the previously assigned ground state rotational band.

2. The energy spacings in two of the even parity rotational bands have been explained in terms of Coriolis interactions, and Coriolis admixtures were determined for each observed state.

3. The α-particle, β- and γ-ray transition probabilities to even parity levels in $^{231}$Pa were calculated with the mixed wave functions, and these results explained what otherwise would have been very anomalous experimental values.

4. More precise values of experimental intensities are needed for low energy electrons in order to better evaluate the effect of the Coriolis interaction in $^{231}$Th β-decay intensities. Quantitative intensity measurements of the low energy $^{231}$Th conversion electron spectrum would be helpful especially for the 17.3 keV transition and also the expected 19.3, 9.3, and 6.4 keV transitions.

5. The $^{230}$Th(α,t)$^{231}$Pa reaction may give the energies of the unobserved 1/2 + (660) and 7/2 + (633) orbitals. This would permit a more precise determination of the Coriolis admixtures and perhaps resolve the discrepancies between theory and experiment in the value of the 1/2 + (660) decoupling parameter and the ratio of the intensities between the 135.77 and 163.16 keV γ rays.

ACKNOWLEDGMENTS

We thank Duane Mosier for his help in setting up and maintaining the electronic equipment, Mrs. Helen V. Michel for her help in the chemical separations of $^{235}$Np, Mrs. Ruth Mary Larimer for her assistance in the target preparations, Martin D. Holtz for the use of his unpublished data on $^{231}$Th decay, Sven G. Nilsson for his discussion of beta decay, and the staff of the 88" Cyclotron for the $^{235}$U target irradiation.

One of us (E.B.) expresses his appreciation to the Lawrence Berkeley Laboratory for their hospitality for 3 years, and to the International Atomic Energy Agency and the Pan American Union for the fellowship which maintained him.

## FOOTNOTES AND REFERENCES

*Work performed under the auspices of the U. S. Atomic Energy Commission.

1. E. Browne and F. Asaro, Lawrence Radiation Laboratory Report Nos. UCRL-17989, 1 (1968), and UCRL-18667, 1 (1969).
2. W. Hoekstra and A. H. Wapstra, Phys. Rev. Letters 22, 859 (1969).
3. E. Browne and F. Asaro, UCRL-19530, 3 (1970).
4. E. Browne and F. Asaro, unpublished results compiled by Agda Artna-Cohen in Nucl. Data B6, 225 (1971).
5. E. Browne, Ph.D. Thesis, National University of Cuyo, Bariloche, Argentina, 1970. (In Spanish)
6. L. B. Magnusson, D. W. Engelkemeir, M. S. Freedman, F. T. Porter and F. Wagner Jr., Phys. Rev. 100, 1237A (1955).
7. Chin-Fan Leang, Compt. Rend. 255, 3155 (1962).
8. F. S. Goulding, D. A. Landis and R. H. Pehl, UCRL-17560 (1967).
9. M. Nakamura and R. L. LaPierre, Nucl. Instr. Meth. 32, 277 (1965).
10. J. E. Gindler and D. W. Engelkemeir, Phys. Rev. 119, 1645 (1960).
11. M. A. Preston, Phys. Rev. 71, 865 (1947).
12. F. Asaro, F. S. Stephens, J. M. Hollander and I. Perlman, Phys. Rev. 117, 492 (1960).
13. J. M. Hollander, F. S. Stephens, F. Asaro and I. Perlman, unpublished results (1956) compiled by C. M. Lederer, J. M. Hollander and I. Perlman in the 6th edition of the "Table of Isotopes", John Wiley & Sons, Inc. (1967), and private communication.
14. M. Holtz, unpublished results (1966) compiled by C. M. Lederer, J. M. Hollander, and I. Perlman in the 6$^{th}$ edition of the "Table of Isotopes", John Wiley & Sons, Inc. (1967), and private communication.

15. S. A. Baranov, R. M. Polevoi, Yu. F. Rodionov, G. U. Shiskin and V. M. Shubko, Izvest. Akad. Nauk. SSSR, Ser. Fiz. 24, 261 (1960): Bull. Acad. Sci. USSR Phys. Ser. Columbia Transl. Series 24, No. 3, 241 (1961).

16. R. S. Hager and E. C. Seltzer, Nucl. Data A4, 1 (1968) and C. M. Lederer, UCRL-19980 (1970).

17. J. E. Mack, Rev. Mod. Phys. 22, 64 (1950).

18. F. S. Stephens, F. Asaro and I. Perlman, Phys. Rev. 113, 212 (1959).

19. J. O. Newton, Nucl. Phys. 3, 345 (1957); 5, 218 (1958).

20. F. S. Stephens, F. Asaro and I. Perlman, Phys. Rev. 113, 212 (1959).

21. D. J. Gorman and F. Asaro, Phys. Rev. C3, 746 (1971).

22. J. M. Hollander, W. G. Smith and J. O. Rasmussen, Phys. Rev. 102, 1372 (1956).

23. J. R. Van Hise and D. Engelkemeir, Phys. Rev. 171, 1325 (1968).

24. D. R. Mackenzie and R. D. Connor, Nucl. Phys. A108, 81 (1968).

25. J. Cardona and A. Gizon, Compt. Rend. 263B, 402 (1966).

26. A. Artna-Cohen, Nucl. Data B6, 234 (1971).

27. S. G. Nilsson, Kgl. Danske Videnskab. Selskab, Mat.-Fys. Medd. 29, No. 16 (1955).

28. A. K. Kerman, Kgl. Danske Videnskab. Selskab, Mat.-Fys. Medd. 30, No. 15 (1956).

29. O. Nathan and S. G. Nilsson, "Alpha, Beta and Gamma Spectroscopy", North-Holland, 608 (1965), Ed. Kai Sieghbam.

30. M. E. Bunker and C. W. Reich, Rev. Mod. Phys. 43, 348 (1971).

31. F. S. Stephens, unpublished data (1960) quoted by E. K. Hyde, I. Perlman and G. T. Seaborg in "The Nuclear Properties of the Heavy Elements", Prentice-Hall, 732 (1964).

32. F. S. Stephens, M. D. Holtz, R. M. Diamond and J. O. Newton, Nucl. Phys. A115, 129 (1968).

33. J. Borggreen, G. Løvhøiden and J. C. Weddington, Nucl. Phys. A131, 241 (1969).

34. J. P. Davidson, "Collective Models of the Nucleus", Appendix D, Table of Nilsson Coefficients, Academic Press, Inc. (1968).

35. E. Browne and F. R. Femenia, Comp. Phys. Comm. 2, 331 (1971).

36. A. Bohr, P. O. Fröman and B. R. Mottelson, Dan. Mat. Fys. Medd. 29, 10 (1955).

37. R. C. Pilger, F. S. Stephens, F. Asaro and I. Perlman, unpublished results (1961-1962) quoted by E. K. Hyde, I. Perlman and G. T. Seaborg, in "The Nuclear Properties of the Heavy Elements", Prentice-Hall, 733 (1964).

38. J. K. Poggenburg, H. J. Mang and J. O. Rasmussen, Phys. Rev. 181, 1697 (1969), and J. K. Poggenburg, Theses, UCRL-16187 (1965).

39. P. G. Hansen, H. L. Nielsen, K. Wilsky and J. G. Cuninghame, Phys. Letters 24B, 95 (1967).

TABLE I. α-particle groups emitted by $^{235}Np$.

| PRESENT WORK | | | | PREVIOUS WORK[10] | | |
|---|---|---|---|---|---|---|
| α-particle energy (MeV) | Excited state energy (keV) | Abundance (%) | Hindrance factor | Excited state energy (keV) | Abundance (%) | Hindrance factor |
| 5.105±0.003 | 0 | 1.5±0.2 | $5.1\times10^{2}$ | 0 | 3.8 | $2.5\times10^{2}$ |
| 5.097±0.003 | 8 | ∿0.2 | $3.4\times10^{3}$ | | | |
| 5.048±0.002 | 58 | 1.8±0.3 | $1.8\times10^{2}$ | | | |
| 5.022±0.002 | 84 | 53±8 | 4.3 | 84 | 83.6 | 3.3 |
| 5.004±0.004 | 103 | 24 ∓8 | 7 | | | |
| 4.994±0.004 | 113 | 6 | 2.5×10 | | | |
| 4.937±0.006 | 171 | ∿0.6 | $1.0\times10^{2}$ | | | |
| 4.922±0.002 | 186 | 11.5±0.5 | 4.4 | 176 | 11.8 | 6.1 |
| 4.859±0.003 | 250 | 0.7±0.1 | 2.7×10 | 238 | 0.8 | 3.5×10 |
| 4.806±0.007 | 304 | ∿0.1 | 8×10 | | | |

TABLE II. γ rays measured in coincidence with $^{235}$Np α particles.

| γ-ray energy (keV) | α gate (keV) | Intensity per α gate (%) | α group | Intensity per α group (%) |
|---|---|---|---|---|
| 58.5±0.4 | $\alpha_{304}\rightarrow\alpha_0$ | 0.6±0.2 | | |
| 81.2±0.2 | | 1.5±0.1 | | |
| 84.2±0.1 | | 6.9±0.4 | | |
| 92.2±0.4 ? | | 0.10±0.05 | | |
| 102.2±0.4 | | 0.30±0.06 | | |
| 110.8±0.4 | | 0.09±0.03 | | |
| 125±1 | | 0.07±0.03 | | |
| 165±1 | | 0.05±0.03 | | |
| 185±1 | | 0.04±0.03 | | |
| 58.5±0.4 | $\alpha_{113}\rightarrow\alpha_0$ (1) | 0.72±0.24 | $\alpha_{113}\rightarrow\alpha_{84}$ | 0.75±0.25 |
| 84.2±0.2 | | 6.4±0.5 | $\alpha_{113}\rightarrow\alpha_{84}$ | 6.7±0.5 |
| 81.2±0.3 | $\alpha_{186}\rightarrow\alpha_{171}$ (2) | 11±2 | $\alpha_{186}$ | 16±3 |
| 84.2±0.2 | | 6.4±0.8 | $\alpha_{186}$ | 6.4±0.8 |
| 92.4±0.4* ? | | 1.0±0.5 | | |
| 102.8±0.4 | | 1.2±0.4 | | |
| 110.8±0.6 | | 0.8±0.3 | $\alpha_{171}$ | 27±14 |
| 126±2 ? | | 0.3±0.2 | $\alpha_{186}$ | 0.4±0.3 |

(1) Gate composition: $\alpha_o$(2%), $\alpha_{58}$(2%), $\alpha_{113}\rightarrow\alpha_{84}$(96%)

(2) Gate composition: $\alpha_{113}\rightarrow\alpha_{84}$(25±3%), $\alpha_{171}$(3±1%), $\alpha_{186}$(69±3%), $\alpha_{250}$(∿3%)

*Not shown in Fig. 1-c.

Table III. $^{231}$Th γ-ray energies and relative intensities.

| This work | | Previous Work[14] | | |
|---|---|---|---|---|
| Energy (keV) | Relative intensity | Energy (keV)†† | Relative intensity | Multipolarity* |
| | | 17.21† | | |
| | | 18.07† | | |
| (25.65)‡ | 202 ±20 | 25.6 | | E1 |
| 42.80±0.06 | 0.87±0.10 | 42.8 | 0.7 | |
| 44.1 ±0.3‡‡ | 0.06±0.04 | | | |
| 58.47±0.05 | 7.2 ±0.7 | 58.54 | 6 | E2 |
| 63.7 ±0.2‡‡ | 0.68±0.14 | 63.79† | | M1+E2 |
| | | 68.50† | | E2 |
| 72.66±0.06 | 4.0 ±0.4 | 72.7 | 3.4 | |
| 73.0 ±0.1‡‡ | 0.10±0.04 | | | |
| | | 76.04† | | |
| 81.18±0.05 | 14.2 ±1.4 | 81.22 | 13 | M1 |
| 82.02±0.06 | 7.2 ±0.7 | 82.07 | 7 | M1 |
| (84.17)‡ | 100 | 84.20 | 100 | E1 |
| 89.94±0.05 | 15.3 ±1.5 | 89.94 | 15 | E1 |
| 92.23±0.05(Pa-$K_{\alpha_2}$) | 6.0 ±0.6 | | | |
| 93.0 ±0.1 | 0.50±0.05 | | | E1** |
| 95.87±0.05(Pa-$K_{\alpha_1}$) | 10.3 ±1.0 | | | |
| 99.30±0.05 | 2.1 ±0.2 | 99.27 | 2.1 | E2+M1 |
| 102.30±0.05 | 6.7 ±0.7 | 102.2 | 7 | E1 |
| 105.73±0.10 | 0.14±0.02 | | | |
| 106.58±0.10 | 0.34±0.04 | 106.8 | 0.34 | |
| 107.62±0.10(Pa-$K_{\beta_3}$) | 1.29±0.14 | | | |
| 108.49±0.10(Pa-$K_{\beta_1}$+$K_{\beta_5}$) | 2.43±0.24 | | | |
| 111.59±0.10(Pa-$K_{\beta_2}$) | 0.9 ±0.1 | | | |
| 112.46±0.10(Pa-K → 0) | 0.34±0.04 | 112.6 | 0.29 | |
| 115.5 ±0.2 | 0.04±0.01 | 115.4? | 0.03 | |
| 116.91±0.05 | 0.39±0.04 | 116.8 | 0.38 | E1 |
| 125.10±0.05 | 0.95±0.09 | 124.9 | 1.0 | |

(continued)

Table III (continued)

| This work | | Previous Work[14] | | |
|---|---|---|---|---|
| Energy (keV) | Relative intensity | Energy (keV)†† | Relative intensity | Multipolarity* |
| 134.14±0.08 | 0.42 ±0.05 | 134.0 | 0.42 | |
| 135.77±0.06 | 1.3 ±0.1 | 135.66 | 1.3 | M1 |
| 136.78±0.20 | 0.09 ±0.03 | | | |
| 145.15±0.30 | 0.12 ±0.03 | | | |
| 146.00±0.07 | 0.58 ±0.06 | 145.90 | 0.5 | M1 |
| 163.16±0.06 | 2.6 ±0.3 | 163.10 | 2.4 | M1 |
| 164.94±0.10 | 0.06 ±0.03 | 164.7 | 0.13 | |
| 169.58±0.10 | 0.03 ±0.01 | | | |
| 174.19±0.08 | 0.31 ±0.03 | 174.1 | 0.29 | |
| 183.47±0.07 | 0.57 ±0.06 | 183.4 | 0.5 | |
| 188.77±0.20 | 0.08 ±0.01 | 188.7 | 0.05 | |
| 218.00±0.07 | 0.67 ±0.07 | 218.0 | 0.6 | |
| 236.17±0.07 | 0.18 ±0.02 | 236.1 | 0.13 | |
| 240.4 ±0.2 | 0.0050±0.0005 | | | |
| 242.6 ±0.1 | 0.0130±0.0006 | | | |
| 249.8 ±0.3 | 0.010 ±0.002 | 249.8 | 0.017 | |
| 250.5 ±0.3 | 0.011 ±0.002 | | | |
| 267.80±0.07 | 0.0230±0.0006 | 267.8 | 0.02 | |
| 308.9 ±0.3 | 0.008 ±0.001 | | | |
| 311.0 ±0.1 | 0.054 ±0.005 | | | |
| 318.0 ±0.4 | 0.0020±0.0002 | | | |
| 320.2 ±0.3 | 0.0035±0.0003 | | | |

†Only observed in electron spectroscopy by Hollander, et al.[13]

††Holtz did not report K X-ray energies and abundances. He interpreted the 112.6 keV radiation as a γ ray.

‡Energies in parenthesis were used as standards and taken from ref. (13).

‡‡These γ rays were only observed by us in coincidence experiments.

*From references 13 and 14.

**See section B3.

TABLE IV. Half lives of γ rays above 200 keV assigned to $^{231}$Th.

| γ-ray energy* (keV) | Half life (hours) |
|---|---|
| 218.00 | 25.5 (assumed) |
| 236.17 | 25.3±0.4 |
| (240.4) | 22±2 |
| 242.6 | 26.9±1.2 |
| 249.8 | 26.2±1.1 |
| 250.5 | |
| 267.80 | 25.5±0.6 |
| 308.9 | 24.9±2.8 |
| 311.0 | 25.9±0.8 |
| (318.0) | 39±16 |
| (320.2) | 29.5±3.0 |

*The assignment to $^{231}$Th of those γ rays in parenthesis is somewhat uncertain.

TABLE V. $^{231}$Th γ-γ coincidence results.

| γ-ray energy (keV) | Intensity per γ gate (%) |
|---|---|
| **84 keV γ-gate** | |
| 63.7±0.2 | 0.048±0.016 |
| 72.5±0.1 | 0.40±0.16 |
| 81.1±0.2 | 1.12±0.16 |
| 82.1±0.2 | 0.57±0.12 |
| 89.9±0.1 | 1.20±0.16 |
| 99.4±0.2 | 0.16±0.04 |
| 116.9±0.1 | 0.032±0.016 |
| 134.1±0.2 | 0.032±0.016 |
| 135.7±0.2 | 0.10±0.04 |
| 146.0±0.1 | 0.040±0.016 |
| 163.1±0.1 | 0.18±0.05 |
| 218.0±0.1 | 0.05±0.04 |
| 236.3±0.2 | 0.007±0.004 |
| **218 keV γ-gate** | |
| 84.0±0.1 | 6.6±0.8 |
| 93.3±0.3 | 0.38±0.22 |
| 102.1±0.1 | 3.0±0.4 |

| γ-ray energy (keV) | Intensity per γ gate (%) |
|---|---|
| **81+82 keV γ-gate(1)** | |
| 42.6±0.5* | 0.12±0.10 |
| | 0.36±0.30 (per $\gamma_{82}$) |
| 58.5±0.1 | 0.72±0.16 |
| 63.7±0.2 | 0.30±0.06 |
| 84.2±0.1 | 8.0±1.6 |
| 93.1±0.2 | 0.15±0.03 |
| | 0.23±0.04 (per $\gamma_{81}$) |
| 102.4±0.1 | 2.1±0.4 |
| | 3.1±0.6 (per $\gamma_{81}$) |
| 136.4±0.2 | 0.05±0.02 |
| **90 keV γ-gate** | |
| 44.1±0.3 | 0.24±0.16 |
| 58.5±0.1 | 0.56±0.16 |
| 73.0±0.1 | 0.40±0.16 |
| 84.2±0.1 | 7.4±1.2 |
| **72.7+73.0 keV γ-gate** | |
| 58.5±0.2 | 0.50±0.16 |
| 72.8±0.2 | 0.36±0.06(2) |
| 84.2±0.1 | 6.5±0.8 |
| 89.9±0.1 | 1.12±0.32 |
| **102 keV γ-gate** | |
| 81.2±0.1 | 7.1±0.6 |
| 137.0±0.3 | 0.03±0.01 |
| 145.2±0.3 | 0.04±0.01 |
| 218.0±0.2 | 0.32±0.16 |

*Not shown in the spectrum of Fig. 4c.

(1) Abundance $\gamma_{81}$/Abundance $\gamma_{82}$=2.

(2) This intensity has been divided by 2 as the energy was included in the gate.

TABLE VI. $^{231}$Th transition intensity balance.

| Energy of state(keV) | Transitions into levels Energy(keV) | Abundance(%)[1] | Transitions out of levels Energy(keV) | Abundance(%)[1] | Log ft. for β decay |
|---|---|---|---|---|---|
| 0 | β⁻ | < 10 | | | > 6.8 |
| 9.3 | β⁻ | < 10 | | | > 6.8 |
| | 68.5 | 0.5 | [9.3](2) | [<10](2) | |
| | 93.0 | 0.040 | | | |
| | 308.9 | ∿0.0007 | | | |
| | 311.0 | ∿0.006 | | | |
| 58.47 | β⁻ | < 8 | | | > 6.5 |
| | 25.65 | 72.5 | 58.47 | 79.4 | |
| | 42.80 | 0.13 | | | |
| | 115.50 | 0.04 | | | |
| | 125.10 | 0.084 | | | |
| | 188.77 | 0.006 | | | |
| | 19.3? | < 16 | | | |
| 77.8 | β⁻ | < 10 | | | > 6.5 |
| | 105.23 | 0.011 | 68.5 | 0.6 | |
| | 169.58 | 0.003 | 19.3? | < 16 | |
| | 240.4 | ∿0.0007 | | | |
| | 242.6 | ∿0.002 | | | |
| | [6.4](2) | < 11 | | | |
| 84.17 | β⁻ | ∿63 | | | 5.6 |
| | 17.21 | ∿17 | 25.65 | 72.5 | |
| | 18.13 | 15 | 84.17 | 26.3 | |
| | 89.94 | 1.2 | [6.4](2) | < 11 | |
| | 99.30 | 1.8 | | | |
| | 163.16 | 1.2 | | | |
| | 236.17 | ∿0.02 | | | |
| | 267.8 | ∿0.002 | | | |
| | 134.14 | 0.036 | | | |
| 101.38 | β⁻ | ∿11 | | | 6.3 |
| | 72.66 | 0.36 | 42.8 | 0.13 | |
| | 116.9 | 0.037 | 17.21 | ∿17 | |
| | 250.5 | 0.0007 | | | |
| | 146.0 | 0.33 | | | |
| | 82.02 | 4.7 | | | |
| | [0.9](2) | [<1.5](2) | | | |
| 102.30 | β⁻ | 6±3 | | | 6.6 |
| | 81.18 | 9.2 | [0.9](2) | [<1.5](2) | |
| | 218.0 | ∿0.1 | 18.13 | 15 | |
| | 249.8 | ∿0.001 | 93.0 | 0.040 | |
| | | | 102.3 | 0.53 | |

Continued

TABLE VI. (Continued)

| Energy of state(keV) | Transitions into levels Energy(keV) | Abundance(%)[1] | Transitions out of levels Energy(keV) | Abundance(%)[1] | Log ft. for β decay |
|---|---|---|---|---|---|
| 174.10 | $\beta^-$ | 1.3±0.3 | | | 6.8 |
| | 44.0 | 0.4 | 89.94 | 1.2 | |
| | 73.0 | 0.009 | 72.66 | 0.36 | |
| | | | 115.50 | 0.04 | |
| | | | 174.19 | 0.12 | |
| 183.47 | $\beta^-$ | 14.9±1.7 | | | 5.66 |
| | 63.8 | 0.94 | 81.18 | 9.2 | |
| | 136.78 | ∿0.03 | 82.02 | 4.7 | |
| | | | 99.3 | 1.8 | |
| | | | 183.47 | 0.044 | |
| | | | 125.10 | 0.084 | |
| | | | 105.73 | 0.011 | |
| 218.28 | $\beta^-$ | 0.5±0.4 | 44.0 | 0.4 | 6.8 |
| | | | 106.58 | 0.026 | |
| | | | 116.9 | 0.037 | |
| | | | 134.14 | 0.036 | |
| 247.33 | $\beta^-$ | 3.3±0.4 | 63.8 | 0.94 | 5.73 |
| | | | 135.77 | 0.79 | |
| | | | 146.0 | 0.33 | |
| | | | 163.16 | 1.2 | |
| | | | 169.58 | 0.003 | |
| | | | 188.77 | 0.006 | |
| | | | 73.0 | 0.009 | |

(1) Abundances are per total β-decay processes.

(2) These transitions in brackets were not experimentally observed but inferred.

TABLE VII. Theoretical and fitted values of the parameters used in the energy level calculation.

| Parameters | Fitted value | Theoretical value |
|---|---|---|
| * $E_{1/2}$ | 400 keV | 200 keV |
| * $E_{3/2}$ | 0 keV | 0 keV |
| $E_{5/2}$ | 34.6 keV | 30 keV |
| * $E_{7/2}$ | 700 keV | 700 keV |
| * $E_{9/2}$ | 1,732 keV | 1,732 keV |
| † $A_{1/2\ 3/2}$ | -44.4 keV | †† -60.7 keV |
| † $A_{3/2\ 5/2}$ | -22.4 keV | †† -59.4 keV |
| *† $A_{5/2\ 7/2}$ | -60 keV | †† -60 keV |
| *† $A_{7/2\ 9/2}$ | -52 keV | †† -52 keV |
| $a_{1/2}$ | 3.7 | 6.5 |
| $h^2/2\mathfrak{J}$ | 9.2 keV | 8.4 keV ** |

* Held constant in the calculation

† $A_{K,K+1} = -h^2/2\mathfrak{J} \langle K+1 \mid j_+ \mid K \rangle$.

†† Using $\langle K+1 | j+ | K \rangle$ from Ref. 30, and $\frac{\hbar^2}{2\mathfrak{J}} = 9.2$ keV

** From the even - even adjacent nuclei.

TABLE VIII. Admixtures in the wave functions of observed even-parity states in $^{231}Pa$

| Energy (keV) | Spin | Admixtures | | | | |
|---|---|---|---|---|---|---|
| | | 9/2 + (624) | 7/2 + (633) | 5/2 + (642) | 3/2 + (651) | 1/2 + (660) |
| 84.17 | 5/2 | 0 | 0 | 0.607 | 0.765 | 0.217 |
| 101.38 | 7/2 | 0 | 0.162 | 0.709 | 0.668 | 0.156 |
| 102.30 | 3/2 | 0 | 0 | 0 | 0.990 | 0.138 |
| 111.62 | 9/2 | 0.0189 | 0.209 | 0.654 | 0.665 | 0.292 |
| 183.47 | 5/2 | 0 | 0 | 0.794 | -0.571 | -0.210 |
| 247.33 | 7/2 | 0 | 0.190 | 0.660 | -0.700 | -0.205 |

TABLE IX. Reduced M1 electromagnetic transition probability ratios for even parity states in $^{231}$Pa.

| $B_{\gamma f}/B_{\gamma f'}$ | $I_i \longrightarrow I_f, I_{f'}$ | Theoretical value Pure state | Theoretical value Mixed state | Experimental value |
|---|---|---|---|---|
| $B_{82}/B_{81}$ | 5/2 7/2,3/2 | 0.0714 | 0.29 | 0.49 ± 0.07 |
| $B_{99}/B_{81}$ | 5/2 5/2,3/2 | 0.428 | 0.01 | 0.02 |
| $B_{135.7}/B_{163}$ | 7/2 9/2,5/2 | 0.156 | 0.22 | 0.87 ± 0.12 |
| $B_{146}/B_{163}$ | 7/2 7/2,5/2 | 0.71 | 0.30 | 0.31 ± 0.05 |

TABLE X. Experimental and theoretical α-decay hindrance factors and β-decay ft values for even parity states in $^{231}Pa$.

| Level energy (keV) | Spin | Experimental α hindrance factor | Calculated α hindrance factor $a_{3/2}$=0.1,N=2.42 | $a_{3/2}$=0.2,N=2.87 | Experimental β(ft×10$^{-5}$) | Calculated β (ft×10$^{-5}$) Pure state | Mixed state[a] |
|---|---|---|---|---|---|---|---|
| 84.17 | 5/2 | 4.3 | 5.7 | 4.3 | ∿4.3 | 63 | 5.5±0.2 |
| 101.38 | 7/2 | 7 | 14 | 11 | ∿20 | 381 | 4.7±0.1 |
| 102.30 | 3/2 | >420 | 1,109 | 251 | $40^{+40}_{-13}$ | 27 | 40 (norm) |
| 111.62 | 9/2 | 25 | 38 | 27 | | | |
| 183.47 | 5/2 | 4.4 | 4.4 (norm) | 4.4 (norm) | 4.6±0.5 | 4.6(norm) | 4.6 (norm) |
| 247.33 | 7/2 | 27 | 22 | 23 | 5.4±0.6 | 11.5 | 5.6±0.3 |
| 304 | 9/2 | 80 | 62 | 75 | | | |

(a) The listed errors reflect only the uncertainty in $U_{3/2}$ and $U_{5/2}$ caused by the experimental errors in the β populations to the 102.30 and 183.47 keV levels.

## FIGURE CAPTIONS

Fig. 1. a) $^{235}$Np α-particle spectrum.

b) $^{235}$Np ($\alpha_{304} \rightarrow \alpha_0$) - γ coincidence spectrum.

c) $^{235}$Np ($\alpha_{113} \rightarrow \alpha_0$) - γ coincidence spectrum.

d) $^{235}$Np ($\alpha_{186} \rightarrow \alpha_{171}$) - γ coincidence spectrum.

------ accidental spectrum due to U-KX rays from the electron-capture decay of $^{235}$Np.

Fig. 2. $^{231}$Th γ-ray singles spectrum.

Fig. 3. Portion of $^{231}$Th γ-ray spectrum from Fig. 2 shown in greater detail.

Fig. 4. $^{231}$Th γ-γ coincidence spectra.

a) ($\gamma_{84}$-γ) coincidence spectrum.

b) ($\gamma_{218}$-γ) coincidence spectrum.

c) (($\gamma_{81}$ + $\gamma_{82}$)-γ) coincidence spectrum.

(*) Peaks due to accidental coincidences and/or coincidences with the Compton tails of higher energy γ rays contained in the gate.

Fig. 5. $^{231}$Th γ-γ coincidence spectra.

a) ($\gamma_{102}$-γ) coincidence spectrum.

b) ($\gamma_{72.7}$-γ) coincidence spectrum.

c) ($\gamma_{90}$-γ) coincidence spectrum.

(*) Peaks due to accidental coincidences and/or coincidences with the Compton tails of higher energy γ rays contained in the gate.

Fig. 6. $^{235}$Np alpha decay scheme.

Fig. 7. $^{231}$Th decay scheme.

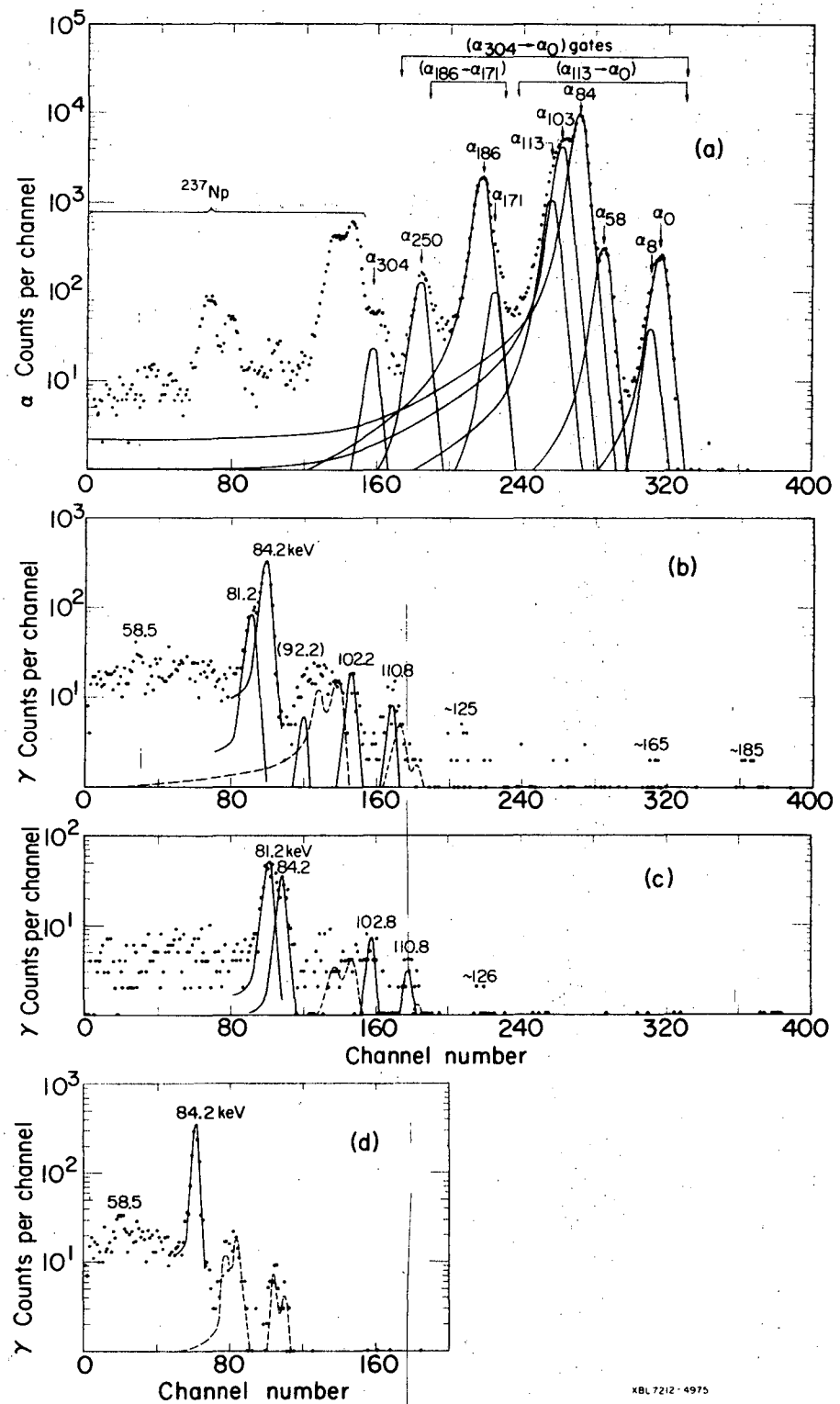
(a)
α Counts per channel
(α304→α0) gates
(α186→α171)
(α113→α0)
237Np
α304
α250
α186
α171
α113
α103
α84
α58
α8
α0
(b)
γ Counts per channel
84.2keV
81.2
58.5
(92.2)
102.2
110.8
~125
~165
~185
(c)
γ Counts per channel
81.2keV
84.2
102.8
110.8
~126
Channel number
(d)
γ Counts per channel
84.2 keV
58.5
Channel number
XBL 7212-4975

Fig. 1

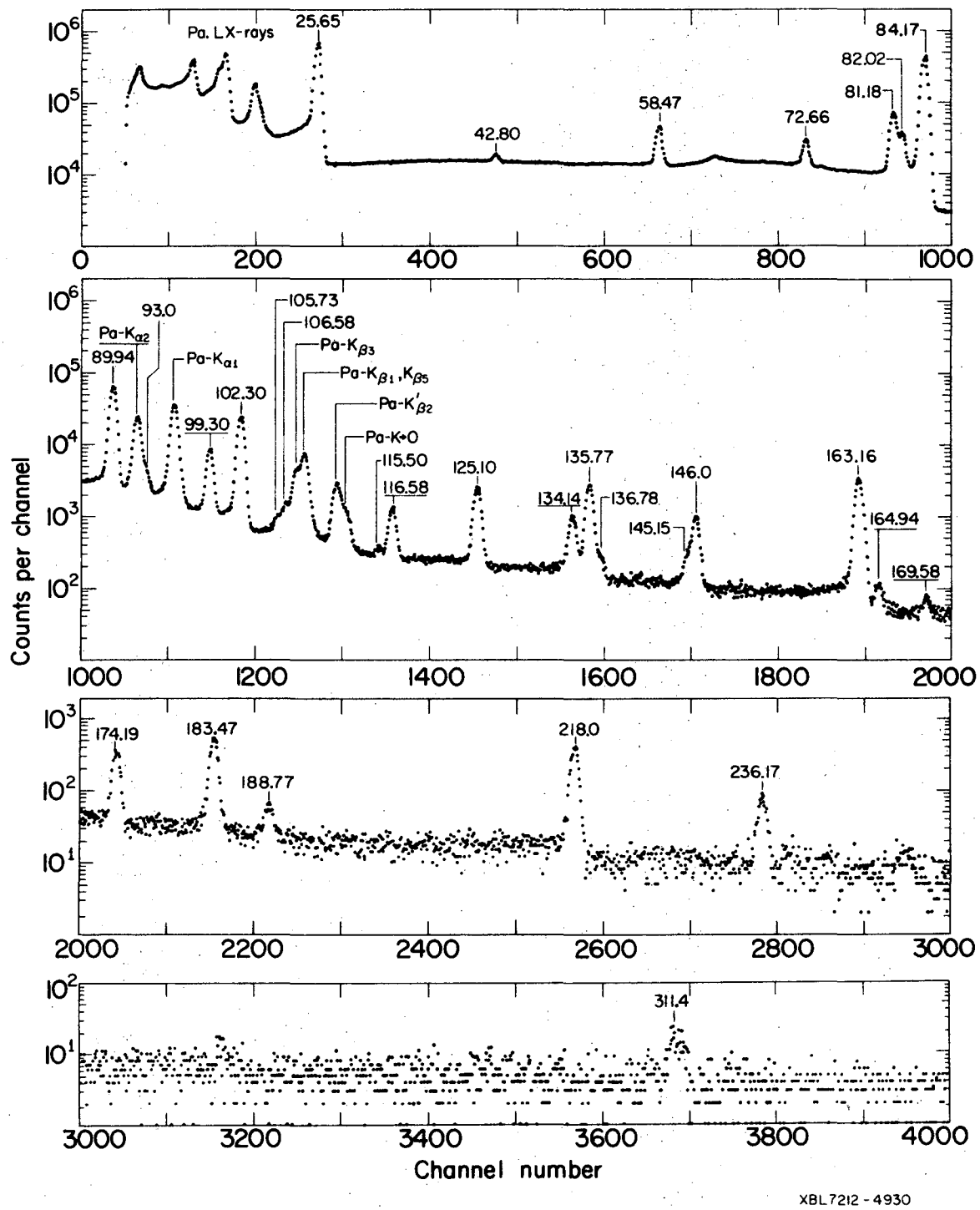
Pa. LX-rays
25.65
42.80
58.47
72.66
81.18
82.02
84.17
93.0
Pa-Kα2
89.94
Pa-Kα1
99.30
102.30
105.73
106.58
Pa-Kβ3
Pa-Kβ1,Kβ5
Pa-K'β2
Pa-K+0
115.50
116.58
125.10
134.14
135.77
136.78
145.15
146.0
163.16
164.94
169.58
174.19
183.47
188.77
218.0
236.17
311.4
Counts per channel
Channel number
XBL7212-4930

Fig. 2

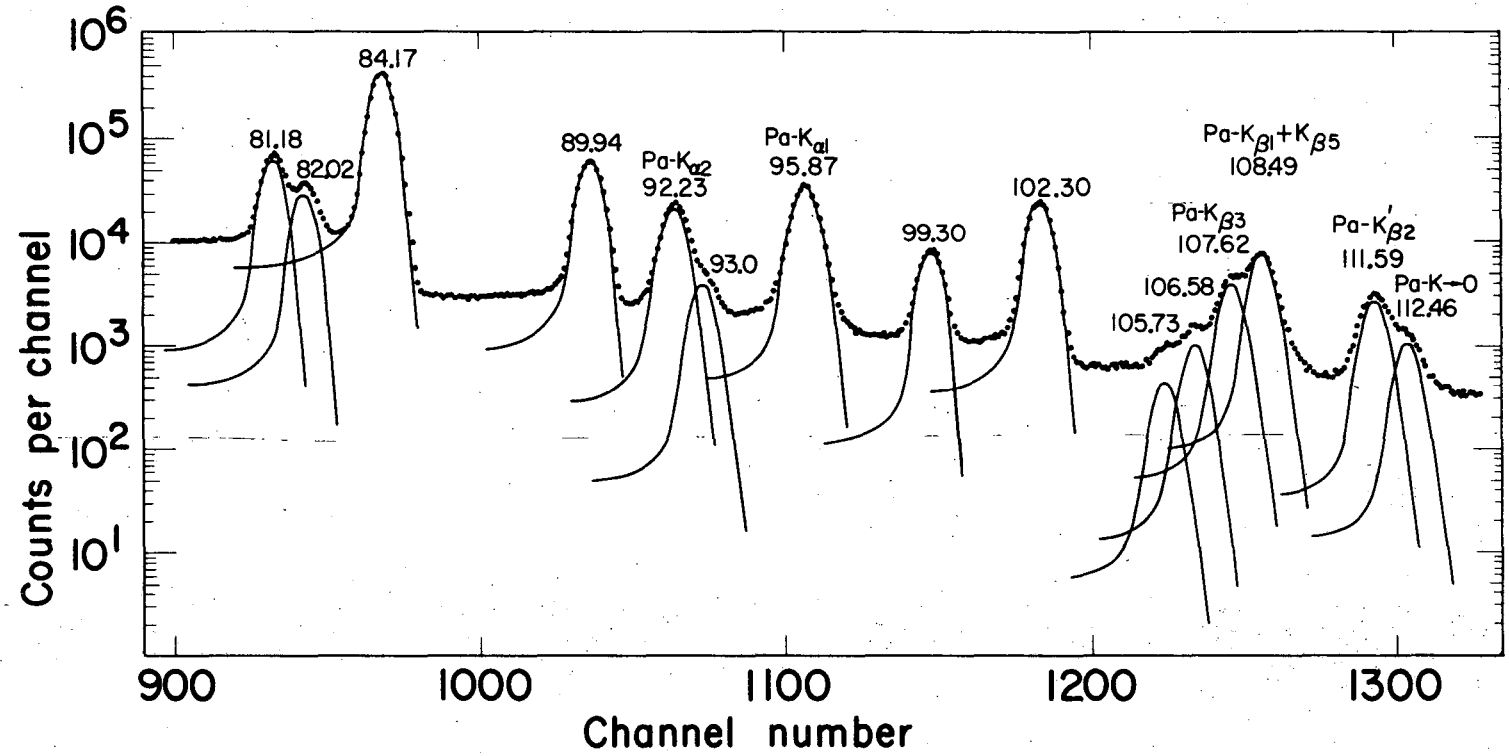
Counts per channel
Channel number
81.18
82.02
84.17
89.94
Pa-Kα2
92.23
93.0
Pa-Kα1
95.87
99.30
102.30
105.73
106.58
Pa-Kβ3
107.62
Pa-Kβ1+Kβ5
108.49
Pa-K'β2
111.59
Pa-K→O
112.46
XBL 7212-4977

Fig. 3

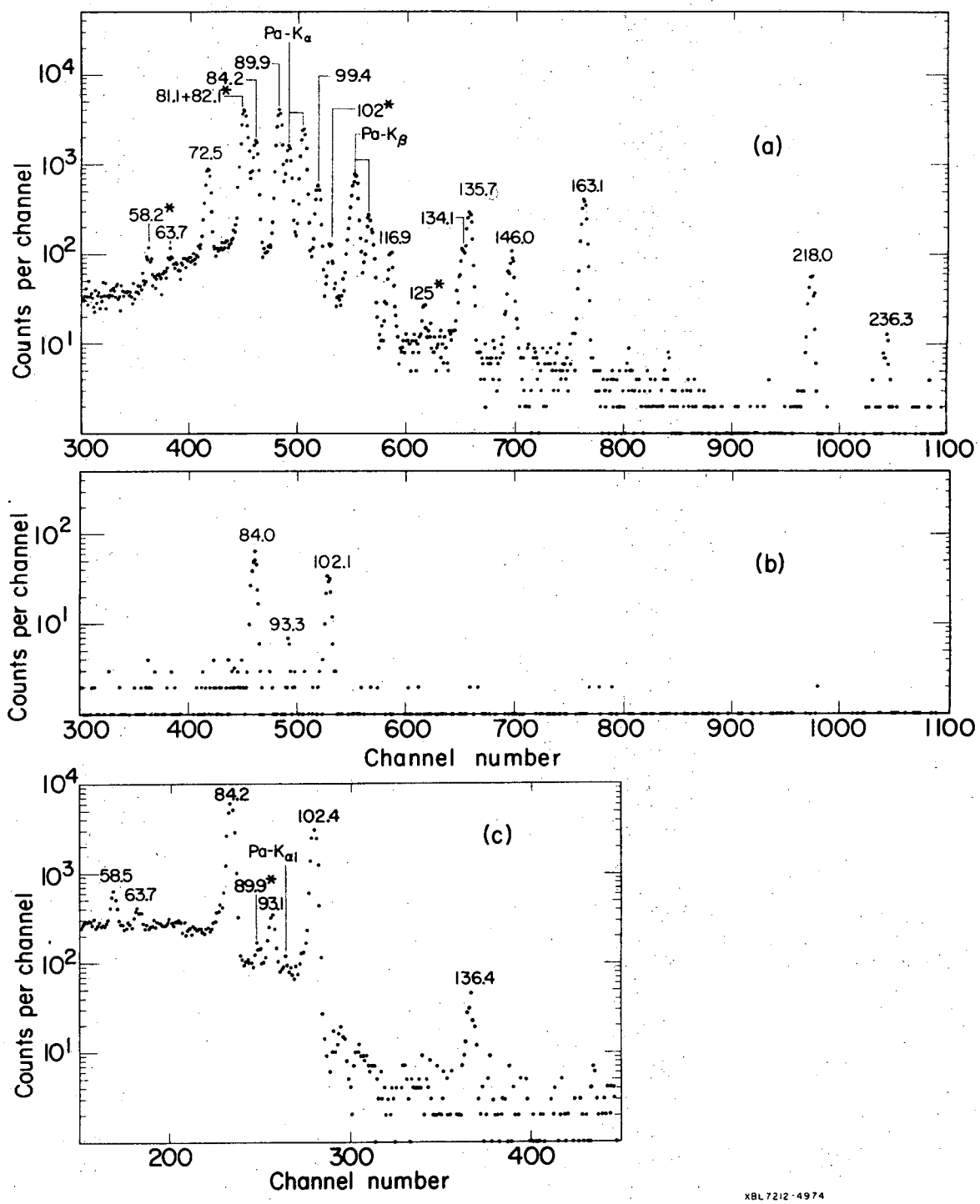
Pa-Kα
89.9
84.2
81.1+82.1*
99.4
102*
Pa-Kβ
72.5
58.2*
63.7
116.9
134.1
135.7
146.0
163.1
125*
218.0
236.3
(a)
Counts per channel
84.0
102.1
93.3
(b)
Channel number
84.2
102.4
Pa-Kα1
(c)
58.5
63.7
89.9*
93.1
136.4
Counts per channel
Channel number
XBL7212-4974

Fig. 4

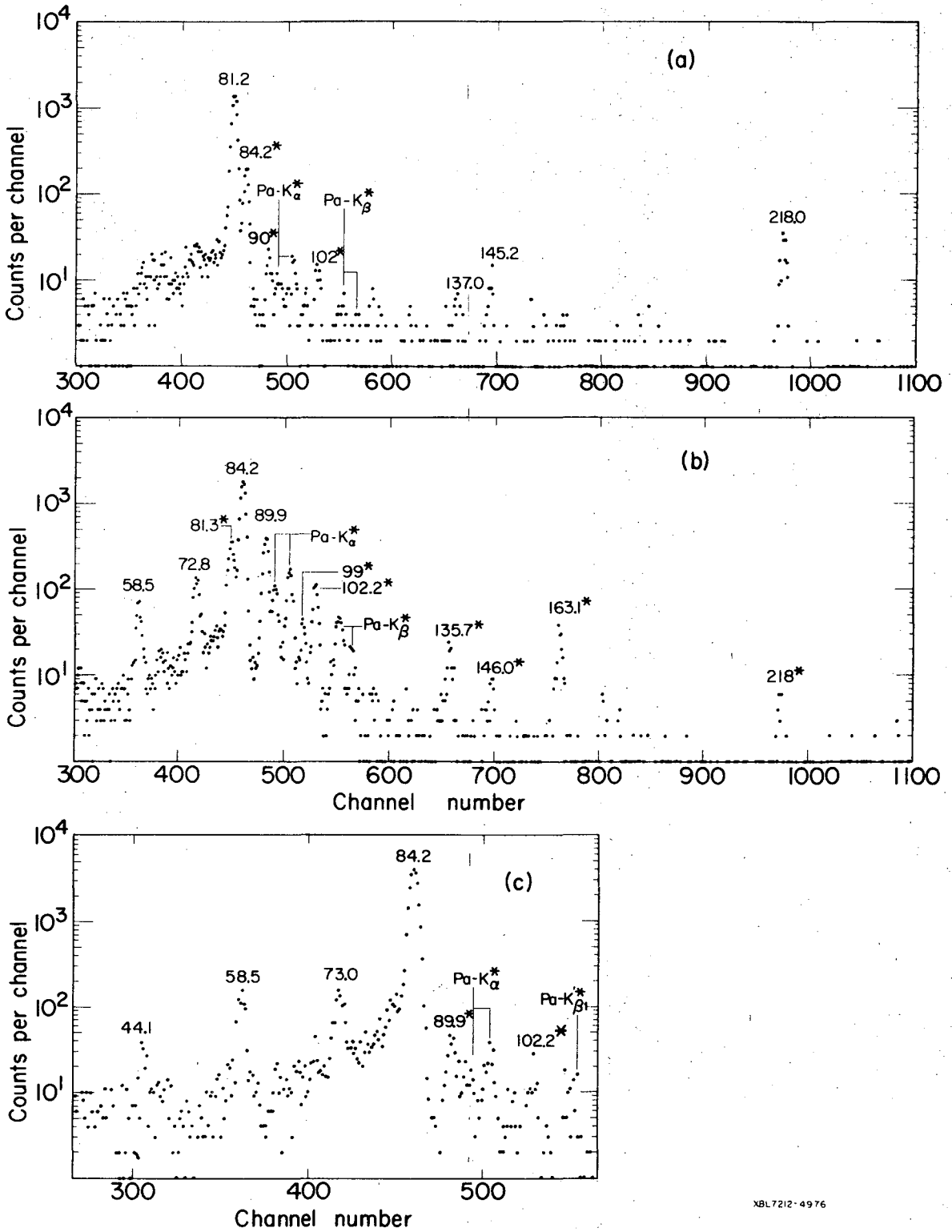
(a)
81.2
84.2*
Pa-Kα*
Pa-Kβ*
90*
102*
145.2
137.0
218.0
Counts per channel
(b)
84.2
81.3*
89.9
Pa-Kα*
72.8
58.5
99*
102.2*
Pa-Kβ*
135.7*
163.1*
146.0*
218*
Counts per channel
Channel number
(c)
84.2
58.5
73.0
Pa-Kα*
Pa-Kβ1*
44.1
89.9*
102.2*
Counts per channel
Channel number
XBL7212-4976

Fig. 5

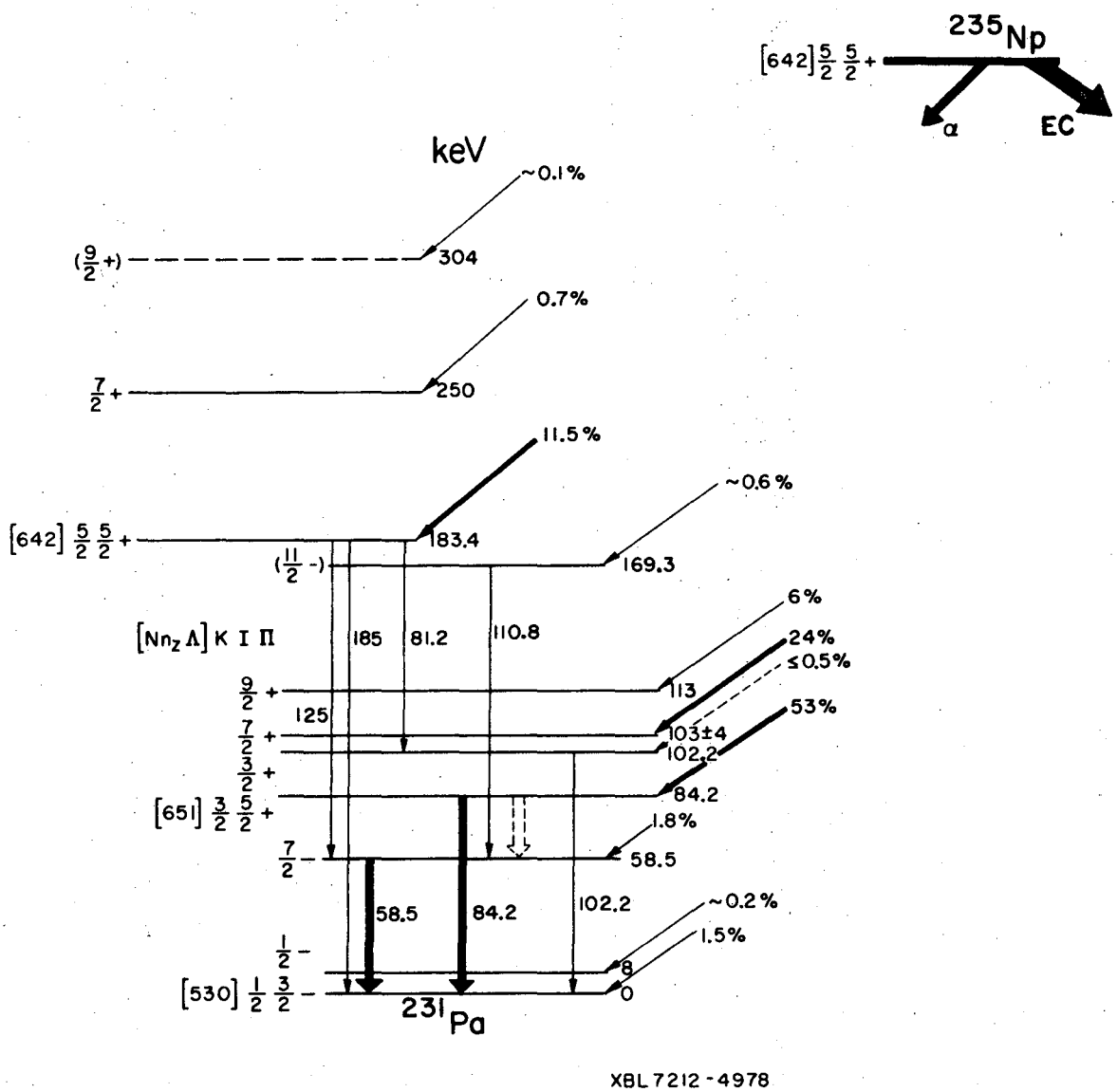
235Np
[642] 5/2 5/2 +
α
EC
keV
~0.1%
(9/2 +)
304
0.7%
7/2 +
250
11.5%
~0.6%
[642] 5/2 5/2 +
183.4
(11/2 -)
169.3
[Nnz Λ] K I Π
185
81.2
110.8
6%
24%
≤0.5%
9/2 +
113
125
7/2 +
103±4
53%
3/2 +
102.2
[651] 3/2 5/2 +
84.2
1.8%
7/2 -
58.5
58.5
84.2
102.2
~0.2%
1.5%
1/2 -
8
[530] 1/2 3/2 -
0
231Pa
XBL 7212-4978

Fig. 6

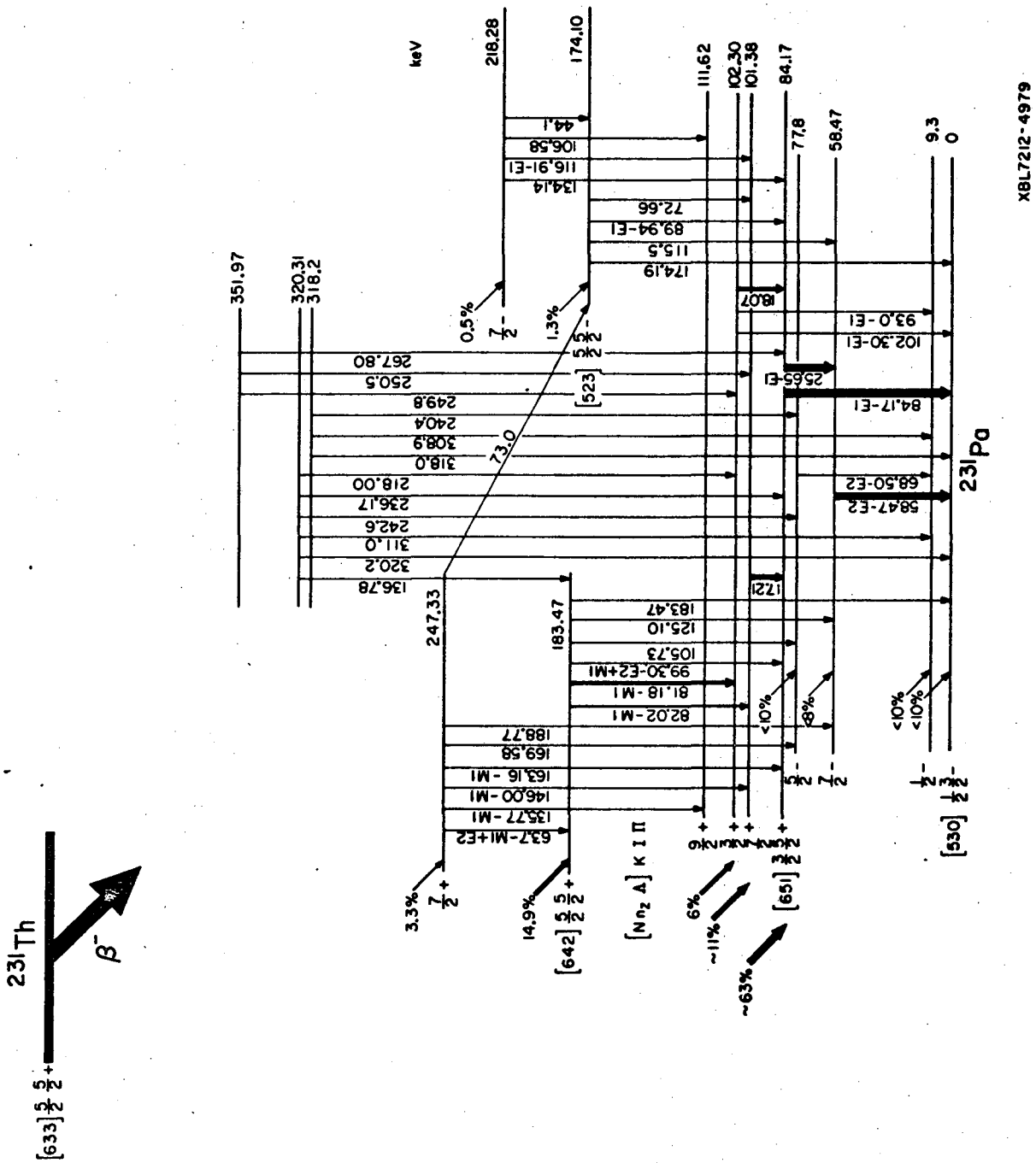
231Th
β⁻
[633] 5/2 5/2+
keV
351.97
320.31
318.2
218.28
174.10
111.62
102.30
101.38
84.17
77.8
58.47
9.3
0
0.5%
1.3%
3.3%
14.9%
6%
~11%
~63%
73.0
[523]
[642]
[651]
[530]
231Pa
XBL7212-4979

Fig. 7

LEGAL NOTICE

*This report was prepared as an account of work sponsored by the United States Government. Neither the United States nor the United States Atomic Energy Commission, nor any of their employees, nor any of their contractors, subcontractors, or their employees, makes any warranty, express or implied, or assumes any legal liability or responsibility for the accuracy, completeness or usefulness of any information, apparatus, product or process disclosed, or represents that its use would not infringe privately owned rights.*

*TECHNICAL INFORMATION DIVISION*
*LAWRENCE BERKELEY LABORATORY*
*UNIVERSITY OF CALIFORNIA*
*BERKELEY, CALIFORNIA 94720*